

**MODELLING VARIABILITY IN THE SOUTH
WEST INDIAN OCEAN AND ITS
INFLUENCE ON SOUTH AFRICA'S
CLIMATE**

**CJC Reason • J Hermes • A Singleton •
JRE Lutjeharms**

WRC Report No. 868/1/03



Water Research Commission



**Modelling Variability in the South West Indian Ocean and its
Influence on South Africa's Climate**

CJC Reason, J Hermes, A Singleton and JRE Lutjeharms

Department of Oceanography, University of Cape Town

Final Report to the Water Research Commission on Project No 868

*Modelling the Variability in the Agulhas Current System and its Influence on
South Africa's Climate*

Report No 868/1/03
ISBN No 1-77005-068-X

Disclaimer

This report emanates from a project financed by the Water Research Commission (WRC) and is approved for publication. Approval does not signify that the contents necessarily reflect the views and policies of the WRC or the members of the project steering committee, nor does mention of trade names or commercial products constitute endorsement or recommendation for use.

Executive Summary

This research project aimed to use atmospheric and ocean general circulation models to better understand the variability of the South West Indian Ocean, a region known to significantly influence southern African rainfall and also extreme event characteristics in the region. An eddy-permitting regional ocean model was applied towards understanding the mechanisms by which ocean variability in the region may arise. This variability then impacts on regional sea surface temperature which influences evaporation, weather system development, moisture transport over southern Africa and hence rainfall. An atmospheric general circulation model was applied towards studying the influence of warm and cool anomalies in the South West Indian Ocean on southern African seasonal circulation and rainfall pattern. Finally, a regional model was used to model the evolution of an extreme rainfall event over southern South Africa and to investigate the influence of low level moisture emanating from the Agulhas Current region.

In summary, the atmospheric modelling results confirm that the South West Indian Ocean is an important source of moisture for seasonal rainfall over southern Africa, when warmer than average sea surface temperature may have a significant influence on extreme weather evolution and tends to lead to drier (wetter) rainfall seasons over the eastern half of South Africa when cooler (warmer) than average. This information may be particularly useful for seasonal forecasting interpretation and development. The ocean modelling indicated that the southern Agulhas Current is a highly variable region on meso-, seasonal and interannual scales. The associated anomalies in heat transported into the southeast Atlantic by the current may influence the evolution of weather systems approaching southern South Africa as well as influence both winter and summer rainfall variability over the country.

The project was successful in terms of the achievement of its objectives, which were extended to address the influence of the larger South West Indian Ocean region instead of the Agulhas Current region only. The project was also very successful in terms of producing peer-reviewed publications and conference presentations. In addition, two PhD students were supported by the project funds, helping to build local capacity in atmospheric and ocean modelling. Two workshops were held during the project attracting participants from several institutions in South Africa.

Acknowledgements

We thank WRC for funding. Arne Biastoch and Marjolaine Krug assisted with ocean model diagnostics. Ross Murray assisted with AGCM diagnostics. The project benefited from the input of the steering committee members (Profs Tyson, Jury, van Heerden, Hewitson and Dr Rautenbach) as well as international collaborative links with CSIRO Atmospheric and Marine Research, United Kingdom Meteorological Office, Australian National University and the University of Melbourne.

Table of Contents

1. Introduction	1
2. Modelling meso- to interannual variability in the Agulhas Current and inter-ocean exchanges south of Africa using an eddy-permitting model.....	1
3. Modelling the atmospheric response to an idealised SST anomaly in the South West Indian Ocean using a general circulation model	22
4. Using a regional atmospheric model to investigate moisture Sources during the storm of December 1998	32
5. Conclusions and recommendations	47
6. Refereed publications to which this project contributed	47

1. Introduction

This report presents atmospheric and ocean modelling work aimed at firstly, quantifying and better understanding the inherent variability of the South West Indian Ocean region, including the Agulhas Current, and secondly, assessing the potential influence of this ocean variability on South African weather and climate patterns. It builds on numerous previous papers (e.g. Walker, 1990; Mason, 1995; Reason and Mulenga, 1999) that have provided strong observational evidence for a link between sea surface temperatures in the South West Indian Ocean and South African rainfall.

Given this previous work and the underlying premise that variability in the South West Indian Ocean significantly influences atmospheric circulation patterns and rainfall over large parts of South Africa, we begin by considering the inherent variability in the Agulhas Current region as diagnosed from an eddy permitting ocean circulation model. This analysis is then followed by applications of atmospheric models towards better understanding South African weather and climate patterns influenced by the Agulhas Current. A concluding section synthesises the work and provides recommendations for future research.

2. Modelling meso- to interannual variability in the Agulhas Current and inter-ocean exchanges south of Africa using an eddy-permitting model

2.1 Introduction

Exchanges of water south of Africa between the South Indian Ocean and the South Atlantic Ocean are an important component of the global thermohaline circulation (Gordon, 1986) and impact on South African climate (e.g., Reason, 1998). These exchanges are predominantly driven by components of the southern Agulhas Current (Gordon, 1985). They come about through the formation of Agulhas rings at the Agulhas retroflexion (Lutjeharms and van Ballegooyen, 1988) as well as other, smaller exchanges by circulatory features such as Agulhas filaments (Lutjeharms and Cooper, 1996). It has been surmised that a considerable exchange also takes place (Gordon et al., 1987) by throughflow of water masses that are not directly related to any mesoscale dynamics such as eddies, rings or filaments. It has also been suggested that the exchange is not a uni-directional affair, but that a considerable amount of water may recirculate in a gyre connecting the two ocean basins (Gordon et al., 1992). A detailed review of what is known about the flow components of the greater Agulhas Current has been given by Lutjeharms (1996). All these flow elements contribute in various proportions to what amounts to a key part of the global heat balance of the ocean. The rate at which heat and salt is exported to the South Atlantic by Agulhas rings has, for instance, recently been shown in a model (Weijer et al., 1999) to influence the rate of meridional overturning in the North Atlantic.

Estimates of the rate of mass and heat exchange south of Africa have varied and it has been extremely difficult to verify these in any reliable manner. Results to date have been comprehensively reviewed by De Ruijter et al. (1999). Most of the heat flux may be carried by upper and intermediate layers since the temperature and therefore the heat content of these water masses is highest (Valentine et al., 1993), but this makes reliable estimates even more difficult because of the extreme mesoscale variability that has been observed in these layers at the Agulhas retroflexion. Some estimates of heat and salt flux have therefore concentrated on that brought about by a specific component of the system only. In this way the heat flux due to Agulhas ring water (i.e., warmer than 10° C) has been estimated to be 0.945 PW and the salt flux at 78×10^{12} kg/year (Van Ballegooyen et al., 1994). The salt flux due to Agulhas filaments has been estimated as about 9 % of that of rings (Lutjeharms and Cooper, 1996). However, the range of estimates by different authors is substantial (viz. De Ruijter et al., 1999). These differences may be due to dif-

ferent estimation methods used, different assumptions made in calculating the fluxes (e.g., the average number of Agulhas rings shed annually), but may also result from the inherent variability of the system itself on intra-annual, interannual and longer time scales.

Attempts to observe the potential variations in the fluxes in the region have been carried out by placing a line of monitoring instruments on a line across the expected path of Agulhas rings (Duncombe Rae et al., 1996; Garzoli et al., 1996; Garzoli et al., 1997; Goni et al., 1997). In a forthcoming monitoring programme, there are plans to enhance previous efforts by one consisting of a more closely spaced line of moorings, placed closer to the origin of the rings (D. Byrne, personal communication). The results from these observational programmes will contribute towards quantifying the fluxes, but regrettably do not include all aspects. For instance, components such as the Agulhas Return Current, which transports water back into the South Indian Ocean (Lutjeharms and Ansorge, 2001), and the mixing of rings before they reach the moorings, have not been considered so far.

Similar to its predecessors, the KAPEX (Cape of Good Hope Experiment) observational programme was partially motivated by the need to estimate the exchanges between the South Indian and the South Atlantic Oceans and particularly those at intermediate depths (Lutjeharms et al., 1997; Boebel et al., 1997). The results from this float study (e.g. Boebel et al., 2001a; Boebel et al., 2001b; Lutjeharms et al., 2001; Schmid et al., 2001) have, for the first time, shown the extreme complexity and variability of all components of the exchange at intermediate depths in the southern Agulhas Current and South East Atlantic Ocean. Taking into consideration the results from the BEST programme (e.g. Garzoli et al., 1997), as well as recent observations from the MARE (Mixing in Agulhas Rings Experiment; Lutjeharms et al., 2000) which have shown that Agulhas rings extend to the sea floor (C. Veth, personal communication), there are sufficient reasons to expect this variability to extend throughout the whole water column in the extended Agulhas retroflection system.

Given the challenges and uncertainties of observational programmes like those described above, it is clear that model based diagnostics of the inter-ocean fluxes are essential. As a first step in this direction, a model designed especially for the Agulhas system (Biaostoch, 1998), which has already been shown to realistically simulate mesoscale features of the system (e.g. Biaostoch and Krauß, 1999), has been used in this initial study of the inter-ocean heat and volume fluxes and their seasonal to interannual variability. Where possible, these model results are compared with fluxes estimated across WOCE lines southwest of South Africa.

2.2 Data and methods

The results presented below were obtained from a twelve year post-spin up integration of the regional eddy-permitting model of Biaostoch and Krauß (1999) which is based on the Modular Ocean Model (MOM version 2, Pacanowski, 1996) developed from earlier versions of the GFDL global ocean model (Bryan, 1969; Cox, 1984). The model domain extends over the South Indian and South Atlantic Oceans from 65-6.5°S and 60°W to 115°E. Within the SW Indian and SE Atlantic Oceans (20°W - 70°E) of interest here, the horizontal resolution is $1/3^\circ \times 1/3^\circ$ (i.e., eddy-permitting with a grid spacing of 30 x 37 km at 35°S for example), while outside this region it gradually coarsens in the zonal direction to reach 1.2° at the meridional boundaries. This region of finer resolution in the SW Indian and SE Atlantic Oceans allows the model to represent larger mesoscale features like Agulhas rings but not much smaller scale features such as Natal pulses. As discussed in Biaostoch (1998) and Biaostoch and Krauß (1999), the model simulation contains a range (in both size and timing) of cyclonic and anticyclonic eddies. The model Agulhas rings are comparable in size and timing to observations, although the rotation and translation

velocities are towards the lower end of observed values. About 2-4 model rings per year occur at the retroflexion zone, which is less than the observations of Byrne *et al.* (1995) and Duncombe-Rae *et al.* (1996). However, due to splitting and other interactions in the Cape Basin, 4-6 model eddies per year cross the WOCE A11 line in the Cape Basin which is more realistic. The model produces a realistic spatial distribution of eddy kinetic energy, although its magnitude tends to be too low in mid- to high latitudes compared to observations as is expected for a model of this resolution (Smith *et al.*, 2000). Given these aspects of the model and its resolution, the term "eddy-permitting" has been used in this paper rather than the more commonly used term "eddy-resolving".

In the vertical, there are 29 levels from the surface to a realistic bottom topography (Fig. 1 of Biastoch and Krauß, 1999) that resolves important features like the Walvis and Southwest Indian ridge, Agulhas Plateau and Bank etc. Near the surface, the layers are 15 m thick in order to better resolve the mixed layer and thermocline, and this vertical grid coarsens to 250 m at deep levels. This grid is a compromise between the desire to represent the mesoscale variability of the Agulhas Current system on interannual time scales while allowing regional water mass formation and exchanges to take place without exorbitant computational cost.

A regional model such as this necessarily includes several open boundaries (Drake Passage, Indonesian throughflow, equatorial Indian and Atlantic Oceans, and the SE Indian Ocean south of Australia) where it must be connected to the rest of the ocean. As discussed in Biastoch and Krauß (1999), this is best achieved through means of the open boundary condition formulation of Stevens (1990) so that waves and other disturbances can propagate out of the domain and will not be reflected at the open boundaries. In this formulation, the linearised horizontal momentum equations are used to calculate the baroclinic velocities at the open boundaries so that the vertical current shear may adjust to the local density gradients. Heat and salt are transported out of the domain using a radiation condition plus advection if the normal component of the velocity at the boundary is directed outward. For those boundary points where the normal velocity is into the domain, restoring of temperature and salinity to the monthly climatology of Levitus *et al.* (1994) and Levitus and Boyer (1994) occurs. Information about the barotropic circulation in the rest of the World Ocean is supplied to the model by prescribing the barotropic streamfunction at the open boundaries from the POCM_4A run (Stammer *et al.*, 1996) of the Parallel Ocean Climate Model of Semtner and Chervin (1992).

Horizontal sub-grid scale diffusion and viscosity are parameterised using a biharmonic operator with respective tracer and momentum coefficients $A_h = A_m = -2.5 \times 10^{19} \text{ cm}^4 \text{ s}^{-1}$ which are constant in the eddy permitting part of the domain and then scale according to the third power of the zonal resolution elsewhere. The latter is done because of the strong dependence of numerical stability on the biharmonic coefficients. In the vertical, a constant Laplacian mixing parameterisation is used for both tracers and momentum ($k_h = 0.3 \text{ cm}^2 \text{ s}^{-1}$; $k_m = 5.0 \text{ cm}^2 \text{ s}^{-1}$).

Wind and heat flux forcing derive from the monthly climatology (Barnier *et al.*, 1995) of the ECMWF model for 1986-1988 while the surface salinity is restored on a 50 day time scale to the Levitus *et al.* (1994) climatology. Implementation of the heat fluxes is via the Haney (1971) parameterisation with restoring to an apparent atmospheric temperature using the Han (1984) time and space dependent coefficients. Shortwave radiation is implemented as a direct penetrative insolation and the cube of the friction velocity is used to drive a simple mixed layer model of the Kraus and Turner (1967) type.

The model is initialised with potential temperatures and salinities from the Levitus WOA94 dataset (Levitus *et al.*, 1994; Levitus and Boyer, 1994) and spun up from rest for 30 model years with a time step of 1/2 hour. At this stage, the wind-driven circulation is stationary with a seasonal cycle. There is of course a slow drift remaining in the tem-

perature and salinity (particularly at depth) since the thermohaline circulation takes thousands of years to adjust - achievement of equilibrium conditions at this resolution is impossible with current computing facilities. However, the general circulation and intermediate to upper ocean water masses are well represented. The model has then been integrated for a further twelve years after this spin up and it is the results from this integration that are analysed below.

The results of interest here are heat and volume fluxes averaged over the years of post-spin up along various transects in the region south of Africa and assessment of the meso-scale to interannual variability of these and other parameters. The heat and volume fluxes are calculated from 5-year statistics after the spinup (i.e. for years 31 - 35). Thus, the zonal heat transport through an arbitrary section was calculated from the averaged correlations as

$$a\rho c_p \int_{\phi_S}^{\phi_N} \overline{u\theta} d\phi dz = a\rho c_p \int_{\phi_S}^{\phi_N} \overline{u}\overline{\theta} d\phi dz + a\rho c_p \int_{\phi_S}^{\phi_N} \overline{u'\theta'} d\phi dz$$

where a is the Earth's radius, ρ potential density, c_p specific heat capacity, u zonal velocity, θ the potential temperature between the latitudes ϕ_S and ϕ_N and primes and overbars indicated eddy components and averages respectively. Thus, the total heat transport can be split into the mean flux (first term on the RHS) and an eddy flux (second term). Similar formulae were used for the meridional heat transport and for the volume transports.

2.3 Results

2.3.1 Mean heat and volume transports

The transects along which model volume and heat transports have been calculated in the southern Agulhas Current region together with a general indication of the flux direction are shown in Fig. 2.1 while the annual mean volume transport along these sections is presented in Fig. 2.2 and Table 2.1. Also plotted as contours on Fig. 2.2 is the barotropic streamfunction, highlighting the Agulhas Current, its retroflection back into the SW Indian Ocean and its inertial re-circulation in that basin, the Agulhas Return Current and the Antarctic Circumpolar Current further south.

Fig. 2.2 and Table 2.1 suggest a transport of around 2.9 Sv into the SE Atlantic along 20°E (**section F**) and about 15.5 Sv north through 35°S (**section A**) on the annual mean. It should be emphasized that there is substantial variability in these inter-ocean fluxes on monthly through to interannual time scales. This variability will be discussed in detail later but at this stage it is useful to consider the mean monthly transport through 20°E together with the standard deviation from the mean and the extreme values (Figure 2.3a) as well as the associated time series from which these statistics were derived (Figure 2.3b). While the **mean annual** transport of 2.9 Sv is always to the west through **section F** into the SE Atlantic, it ranges from as much as 12 Sv east from the SE Atlantic to the SW Indian Ocean during the summer of year 34 to almost 16 Sv west into the SE Atlantic during the winter of years 31 and 34 (Figure 2.3b). The standard deviation (Fig. 2.3a) ranges from about 2.4 Sv in winter to about 3.6 Sv in summer. While Fig. 2.3a suggests that the net flow through **section F** is generally only eastwards back into the SW Indian Ocean in summer, it can be seen from the time series in Fig. 2.3b that weak eastward net flow can also occur at other times of the year (e.g. autumn of year 31 and spring of year 33).

Much of the flow west through **section F** re-circulates so that only about 0.3 Sv escapes into the SE Atlantic west of 5°E (**section E**) on the annual mean (Fig. 2.2 and Table 2.1). The southward flow of 61.3 Sv through **section B** east of Cape Agulhas is consistent with the 65 Sv total Agulhas transport estimated by Stramma and Lutjeharms (1997)

from historical hydrographic data. The model indicates that the net return flow through 35°E (**section G**) back into the SW Indian Ocean is 66.5 Sv, and a substantial part of this joins the inertial re-circulation in the SW Indian Ocean that is the major source of the Agulhas Current. For example, Stramma and Lutjeharms (1997) estimate that the inertial re-circulation contributes about 45 Sv to the transport of the Agulhas Current.

The contribution of the upper and intermediate layers to the total depth integrated transports discussed above can be seen from Table 2.2 which lists the transport for the upper 436 m and 436-1575 m layers. It can be seen that roughly half the total transport through **sections B and G** (the Agulhas Current and Return Current respectively) occurs in each of the upper and intermediate layers with only about 3 % and 7 % respectively coming from that part deeper than 1575 m. On the other hand for **section A**, west of South Africa, Table 2.2 implies that at depths beneath 1575 m, there must be a return flow of 8.3 Sv south from the SE Atlantic to balance the excess contributions from the upper and intermediate layers to the total northward transport through this section of 15.5 Sv. For **Section E**, the weak net westward flow of 0.3 Sv comprises 6.5 Sv in the intermediate and 4.8 Sv in the deeper layers since the upper layer flow is 11 Sv to the east on the annual mean. Both **sections A and E** are characterised by shifts in the location of the Agulhas retroflexion and significant ring shedding which makes the diagnosis of the contributions from each layer more complex.

The flux calculations through **sections E, F, G** are sensitive to the southern boundary since this may result in part of the Antarctic Circumpolar Current being included in the transport. Table 2.1 lists the annual and seasonal mean fluxes (the latter to be discussed later) through **sections C, D, E, F, G** re-calculated for the southern boundary located at 43°S and 47°S respectively. As expected, there is considerable sensitivity along these sections but particularly for **sections C, E, F** since these most closely reflect the strong gradients associated with the Agulhas retroflexion and Return Currents and the ambient flow to the south.

The annual mean heat budget averaged over the two boxes south of Africa (Fig. 2.4) indicates that for the western (eastern) box, the ocean loses 0.054 PW to (gains 0.015 PW from) the atmosphere and that it gains (loses) 0.050 PW (0.013 PW) through the excess (deficit) of ocean heat transport into the region. The ocean heat transport differences for the two boxes arise since the net Agulhas Current heat flux (**section B minus A**) into the entire region plus the inflow through **sections C and D** from the south is slightly greater than the net outflow which is mainly due to the Agulhas Return Current and SW Indian Ocean re-circulation through **section G**. Note that there will not be a precise heat balance between the net ocean heat transport and the net exchange with the atmosphere since the diffusive flux has been ignored and there may be a small amount of heat change by the region over the relatively short period of integration due to the slow drift of the thermohaline fields.

Of most interest for this study are the values through **sections E, F and A** along 5°E and 20°E south of Africa and along 35°S west of the southern tip of Africa as these indicate the inter-ocean transfer from the SW Indian to the SE Atlantic Oceans. On the annual mean, there is a net westward transport through **section F** of 0.84 PW (Fig. 2.4 and Table 2.3) but as seen from Fig. 2.5ab (the monthly heat transport through this section with standard deviation and extreme values), this ranges from as much as 1.3 PW west into the SE Atlantic during spring of year 32 to only about 0.35-0.5 PW west during each summer / autumn. Standard deviations range from about 0.1 PW in winter to 0.13-0.17 PW in summer (Fig. 2.5a). Given that the westward flowing Agulhas Current water is much warmer than that further south along **section F**, the net heat transport is always west into the SE Atlantic even if the net volume transport through this section is sometimes east back into the SW Indian Ocean (Figs. 2.3ab). However, further west, this westward Agulhas transport into the SE Atlantic is essentially returned by the retroflec-

tion so that there is in fact an eastward heat transport along 5°E (**section E**) of 0.02 PW (Fig. 2.4 and Table 2.3) on the **annual mean**. (As discussed later, this is only true for summer and autumn - during winter and spring, the heat transport is westwards into the SE Atlantic).

The net 1.9 PW flowing south into the region across 35°S is comprised of 2.93 PW southward transport via the Agulhas Current (**section B**) and, west of Cape Agulhas (**section A**), a northward transport into the South Atlantic of 1.03 PW. The latter value is larger than both the hydrographic estimates (0.02-0.47 PW) of Gordon (1985) and previous model estimates by FRAM (0.51 PW - Thompson *et al.*, 1997) and Semtner and Chervin (1992) (0.6 PW). However, the FRAM heat transport is thought to be too low since it neglects the role of the Indonesian throughflow (Ribbe and Tomczak, 1997). Also, the Semtner and Chervin model does not include the Mozambique Channel leading to a different warm water transport in the southwest Indian Ocean. A review of model and observationally derived heat fluxes is given by de Ruijter *et al.*, (1999); clearly, different model results derive from differences in the model forcing and the parameterisations of the sub-grid scale physics.

Similar to the earlier discussion for the volume transports, there is sensitivity in the transports to the location of the southern boundary (**sections C and D**) (Table 2.3) and the depth integrated transport can be decomposed into upper, intermediate and deep layer contributions (Table 2.4). Along the Agulhas Current dominated **section B**, about 75 % of the net southward heat transport of 2.92 PW occurs in the upper layer, 29 % in the intermediate layer and there is a weak return transport of 0.14 PW (5 %) distributed over the layer below 1575 m. Similar proportions were found for **section G**, dominated by the Agulhas Return Current. These proportions are biased towards the upper layer compared to those discussed above for the volume transports (Table 2.2) due to the water temperature of each layer. Along **section A**, Table 2.4 implies a return southward flow at depth of 0.17 PW while along **section E**, as for the volume transport, there is a significant intermediate layer transport in the reverse (westward) direction to the upper layer so that the net transport is relatively small. Again, the transport here is biased by the significant variability in the location of the Agulhas retroflection.

The fluxes discussed above refer to that resulting from both the eddy component and the mean current. The former is visible mostly in the case of small scale eddies where relatively warm water is transported in one direction on one side of the eddy, and cooler water in another direction on the other side. For Agulhas rings, warm water is trapped within this mesoscale feature and transported to the northwest as the eddy drifts in that direction from the retroflection area into the SE Atlantic. The translation velocity of the Agulhas ring appears in the mean velocity and so the heat transport associated with Agulhas rings will not appear in the eddy component. For the latter, there will only be a contribution to the total heat transport if there is heat exchange with the atmosphere or by diabatic mixing with the surrounding water. Adiabatic heat exchange with the ambient water will appear in the eddy component but not in the total heat transport. As a result, estimates of the direct contribution of the eddy component to the heat transport are not straightforward. However, estimates of the eddy flux were made and reveal that along 20°E (**section F**), there is a net westward transport into the South Atlantic of 0.12 PW (Fig. 2.6) as compared to the total westwards transport integrated along this section of 0.84 PW. These results suggest that in the model, eddy variability (not rings) associated with the southern Agulhas, the retroflection region and the western part of the Agulhas Return Current can make a small but not insignificant contribution to the heat transport into the South Atlantic. Although resolution dependent differences in the model physics and parameterisations preclude a direct linear comparison, it is worth noting that the westward heat transport in a coarser 1 degree resolution version of the model is much smaller than the 0.12 PW noted here, further indicating that eddies are significant for the model heat transport.

2.3.2 Variability in heat and volume fluxes

Figs. 2.7-2.8 show time series and spectra of the heat and volume transports at various locations in the region obtained from the years 31-42 of the integration. Common to all sections is the significant variability ranging from meso- to interannual time scales. Since the model is forced with the same monthly forcing each year, the interannual variability evident in the model arises from internal ocean processes and not from any imposed atmospheric forcing. There are small differences in the significant peaks of the spectra at various locations which are of interest. For example, comparison of the heat flux spectra for the northern half of **section F** (i.e., averaged over 35-40°S and mainly westward flowing) (Fig. 2.7a bottom right panel) with that for the southern half of **section F** (i.e., averaged over 40-45°S and mainly eastward flowing) (Fig. 2.7b bottom right panel), suggests that the annual cycle is slightly stronger relative to the semiannual and meso-scale peaks in the southern half. This suggestion is consistent with earlier work by Matano *et al.* (1998) which relates the stronger annual cycle in the retroreflection region and the weaker manifestation of this cycle in the southern Agulhas Current to the role of bottom topography. However, Matano *et al.* (2001) found a significant annual cycle in the Agulhas Current at 32°S in the POCM simulation while Biastoch and Krauß (1999) discuss seasonal variability of the Agulhas Current and Mozambique Channel flows revealed by the model used in this study. In general, there is a tendency for lower westward transfer into the South Atlantic in summer/autumn and higher in winter/spring, reflecting the seasonal variation in the surface forcing. For example, the corresponding seasonal volume and heat transect values (Tables 2.1, 2.3) to those discussed above for the annual mean indicate that there is a net westward heat export into the South Atlantic across **section F** (20°E) between Africa and 45°S of 1.00 PW in winter, 0.96 PW in spring, 0.66 PW in summer and 0.74 PW in autumn. Volume transports range from a net westward flow of 2.5 Sv in autumn, 3.5 Sv in spring, and 8.5 Sv in winter to a net eastward transport of 3.1 Sv in summer. Upstream in **section B** east of Cape Agulhas along 35°S, the southward transports range from 57.6 Sv (2.83 PW) in summer, 59.1 Sv (2.79 PW) in autumn to 63.6 Sv (3.00 PW) in winter and 64.7 Sv (3.08 PW) in spring (Table 2.1). Similar seasonal variations in volume transport were noted further upstream at 32°S by Biastoch *et al.* (1999). As indicated in Table 2.1, this section (**B**) has the weakest amplitude in the annual cycle as it essentially reflects the tight core of the Agulhas Current. The amplitude is much greater for **sections C, D, E, G** which are less constrained by bottom topography and, hence, can respond to the seasonal variations in not just the local winds but also those across the basin (Matano *et al.*, 1998). It is largest for the two South East Atlantic **sections A and C** because the variability here is also contributed to by seasonal shifts in the position of the Agulhas retroreflection itself.

For the SE Atlantic **section A** west of South Africa, the timing and magnitudes of the seasonal signal differ somewhat from those already described along **section F** south of Africa. For **section A**, the strongest northward heat transport into the Atlantic occurs in spring (1.11 PW) and autumn (1.10 PW) followed by winter (0.97 PW) and summer (0.92 PW) (Table 2.3). The magnitude of the annual cycle along **A** is of order 10 % as compared to around 20 % through **F**. It is possible that the timing differences result from the mid-latitude Semiannual Oscillation being more prominent for the **section A** west of South Africa than for **section F** south of South Africa. This may arise because **section F** mainly reflects the forcing over the subtropical South Indian Ocean whereas that along **A** in the South East Atlantic is more sensitive to midlatitude wind variability consistent with the suggestion of Matano *et al.* (1998). Heat fluxes through **section A** mainly occur via the passage of Agulhas rings shed off the retroreflection region further south, and the seasonal variability of this process in the model is less pronounced than that in the flow upstream through **section F**.

Estimates from hydrographic data along the diagonal WOCE line SR02 southwest from Cape Town have recently been made for two summer cruises that took place in 1990 and 1993 respectively. Although these diagonal lines do not directly correspond to the model lines they are of interest as they enable one to see whether the model appears consistent with observational estimates. For the 1990 cruise from 18° 27' E, 35° 19' S (i.e. about 100 km south of Cape Town) southwest to 9° 29' E, 44° 53' S, a heat transport of 0.51 PW was calculated. For the 1993 cruise from Cape Town southwest to 45 S, 8.5°E, a value of 0.6 PW was obtained. These estimates were obtained using the inverse box method (e.g. Wunsch, 1996) from stations spaced about 30-50 nautical miles apart and assuming the level of no motion to be 2000 m. They suggest firstly, that the model summer estimate of 0.66 PW (with standard deviation of 0.13 PW in March to 0.17 PW in January - Fig. 2.3a) heat transport west through **section F** at 20°E is reasonable, and secondly, that there may be substantial interannual variability in interocean heat transports in the real ocean. The latter is consistent with Fig. 2.7 which indicates substantial interannual variability in the model **section F**.

The semiannual signal seen in the spectra and timeseries **through F** (Fig. 2.7) seems to be a feature of the Agulhas and Agulhas Return Current, spectral energy at this time scale does not show up in the heat and volume transports averaged along the other sections (e.g. **E**, Fig. 2.8). A semiannual signal in winds and mean sea level pressure is a prominent feature of the Southern Hemisphere midlatitudes (van Loon and Jenne, 1972) and relates to the semiannual variations in the temperature gradient between the subtropics and the mid- to high latitude regions influenced by surface ice cover. Semiannual signals can also be diagnosed in the tropical Indian Ocean (Bjorndal and Morrow, 2001) and relate to Rossby waves propagating at this period. Matano *et al.* (2001) diagnosed a strong semiannual signal in the South Equatorial Current in the POCM simulation with a weaker signal on this timescale in the East Madagascar and Agulhas Currents. It is unknown whether this semiannual Agulhas and Agulhas Return Current signal (Fig. 2.7) derives from the Southern Hemisphere semi-annual oscillation in mid- to high latitude winds and surface pressure or from that in the South Equatorial and East Madagascar Currents or whether these are related to each other.

Comparison of the spectra averaged along 20°E (**section F**) with that along 5°E (**section E**) indicates that there are some significant events occurring in the latter which do not appear on the upstream section (Figs. 2.7-2.8). These result from seasonal variability in the longitudinal position of the Agulhas retroflexion zone itself which directly influences **section E** (Fig. 2.8) and leads to the spectral peak near 12 months dominating at this section. Meridional shifts in this retroflexion zone also occur and this contributes towards shifts in the sign of the transport between generally west and north into the SE Atlantic to events of 1-3 month duration when the transport is reversed back into the SW Indian Ocean. By contrast, the northern (southern) half of **section F** along 20°E, 35-40°S (40-45°S) always shows heat transport west into (east from) the SE Atlantic Ocean although its magnitude is highly variable on eddy to interannual scales (Fig. 2.7).

For the **section E** (Fig. 2.8), the spectrum is dominated by the annual cycle (e.g., shifts in the retroflexion) and by variability at meso- or eddy time scales. Note that as already discussed, this eddy peak does not include Agulhas rings as their translation velocity is reflected in the mean not eddy component. The mesoscale peak is at 110 days similar to that found by Biastoch and Krauß (1999) for a 5 year integration of the model and which they attribute to baroclinic instability in the mean flow.

2.4 Variability in the northern Agulhas Current and Mozambique channel

The main focus of the work has been on the southern Agulhas system; however, it is pertinent to summarise at this point earlier work by the authors (Biastoch *et al.*, 1999) that highlights the potential significance of flow in the Mozambique Channel to the seasonality in the greater Agulhas Current system. It had previously been demonstrated

(Stramma and Lutjeharms, 1997) that at least 8% of the baroclinic volume flux of the Agulhas Current derives from the Mozambique Channel. Furthermore it is feasible that the changes in monsoonal winds north of about 15°S might provide strong seasonal forcing for currents near and in the Mozambique Current (Maltrud *et al.*, 1998).

Figure 2.9 shows the seasonality exhibited by the model, firstly in the Agulhas Current (at 32°S). The weakest transport here is in January and March with the maximum in October/November. There is strong evidence of seasonality in the Mozambique Channel with the max southward transport occurring in August. However, there is little evidence of seasonality in the East Madagascar Current. The lag between the Mozambique Channel and the Agulhas Current (2-3 months) suggests an advective link between the seasonal signal of the two.

Harris (1972) showed that the contribution to the flux of the Agulhas Current, from the Mozambique Channel, consists largely of Tropical Surface Water (TSW). Further work with the model demonstrated that, at 20°S, the salinity minimum (corresponding to the model TSW) is evident from May to August. At 24°S the minimum can be seen in July and August and at 31°S, the Agulhas Current Proper, there is a weak signature from September to December. Taking a typical current speed for the inshore edges of the Agulhas Current, estimates of the time for this water to be advected between 20-24°S is 23 days and 24-31°S is 32 days. These estimates appear consistent with the advective time lags. Unfortunately hydrographic data in the appropriate spacing is sparse and hence currently available observations are inadequate to confirm the hypothesis that seasonal variations in the transport of TSW through the Mozambique channel contribute to the seasonality of the Agulhas Current. However, they are not inconsistent with this concept and their sparsity re-inforces the need for an extended field study in this important region.

Figure 2.10 demonstrates a plausible mechanism as to why there is seasonality in the flow through the Mozambique Channel. The core of the South Indian anticyclone moves northward during austral winter and the associated barotropic transport can flow north of Madagascar and can be driven into the Mozambique Channel. 25% of the total flow into the Channel is due to Ekman Transport associated with Southeasterly winds, northeast of Madagascar. This flow transports TSW from the Indian Ocean into the channel during winter with advection of this signal in the Agulhas Current by spring.

The transport does not extend into the Mozambique Channel during summer as the anticyclone lies too far to the south and the net southward transport in the Channel is near zero. 2 to 3 months later the Agulhas Current receives a greater proportion of its water from the South West Indian Ocean gyre.

2.5 Summary and conclusions

This study has used output from a regional eddy-permitting model to consider the heat and volume transports between the SW Indian and SE Atlantic Oceans south of Africa as well as their seasonal and interannual variability. The model estimate of 1.03 PW (standard deviation 0.2 PW) flowing north into the SE Atlantic through **section A** along 35°S is larger than previous hydrographic estimates (0.02-0.47 PW - Gordon (1985)) and model calculations (0.51 PW by Thompson *et al.* (1997) and 0.6 PW by Semtner and Chervin (1992)); however, as discussed in Section 3.1 both these models left out potentially important factors such as the Indonesian throughflow and the Mozambique Channel flow. The model summer transport value through **section F** along 20°E south of Africa of 0.66 PW (standard deviation ranging from 0.13 PW in March to 0.17 PW in January) appears consistent with recent hydrographic estimates of 0.51 PW (1990 data) and 0.6 PW (1993 data).

Considerable attention has been paid herein to the model variability which refers to only that generated internally through ocean processes since the monthly forcing is repeated each year. Observations are sparse but those that exist do suggest that this model is able to realistically represent the circulation and its mesoscale variability; hence, there is a level of confidence in the model results. Further confidence follows from a qualitative visual comparison (not shown) between virtual floats released in the model and the limited number of observational float tracks available from KAPEX.

The model results support the suggestions from previous observational and model work that the southern Agulhas Current region is highly variable on meso-, seasonal and inter-annual time scales. The study has focussed on variability generated through ocean processes; how it might change under the full spectrum of atmospheric variability (which is not represented in the monthly climatology used to drive the model) is not known. Observations, although limited, indicate that the region is highly variable from one year to the next and therefore, were the model forced with the observed winds for particular years rather than a monthly climatology, one would naturally expect the simulated ocean variability to be even greater than analysed herein. These observations also suggest that this variability (as expressed through regional SST anomalies) is significant for regional weather and climate patterns; thus, a better assessment of the interocean exchanges and its influence on SST is important beyond its contribution to the global thermohaline circulation. For example, studies by Walker (1990), Mason (1995), Reason (1998), Reason and Mulenga (1999), and Rouault *et al.* (2001) have specifically related South African intraseasonal and interannual rainfall variability as well as the intensity of local storms to SST anomalies in the Agulhas Current region.

Given this evidence for the potential significance of heat exchange between the South Indian and South Atlantic Oceans on not just the global thermohaline circulation but also for regional weather and climate variability, there is considerable motivation for more comprehensive studies of this inter-ocean exchange. Studies using higher resolution models which are better able to capture Natal Pulses, smaller scale eddies and other smaller mesoscale features would be necessary to get a better idea of the contribution of eddy features to this heat exchange. A more detailed model-based study along these lines is planned and it is hoped that this, in conjunction with available observational estimates, will provide a more extensive understanding of the inter-ocean exchange south of Africa and its variability.

2.6 References

- Barnier, B., Siefridt, L., Marchesiello, P., 1995. Thermal forcing for a global ocean circulation model from a three-year climatology of ECMWF analyses. *Journal of Marine Systems*, 6, 363-380.
- Biastoch, A., 1998. Zirkulation und Dynamik in der Agulhasregion anhand eines numerischen Modells. *Berichte aus dem Institut für Meereskunde an der Christian-Albrechts-Universität Kiel* 301, pp. 118.
- Biastoch, A., Krauß, W., 1999. The role of mesoscale eddies in the source regions of the Agulhas Current. *Journal of Physical Oceanography* 29, 2303-2317.
- Biastoch, A., C.J.C. Reason, J.R.E. Lutjeharms and O. Boebel, 1999: The importance of the Mozambique Channel for the seasonality of the Agulhas Current. *Geophysical Research Letters*, 26, 3321-3324.
- Birol, F., Morrow, R., 2001. Source of the baroclinic waves in the southeast Indian Ocean. *Journal of Geophysical Research* 106, 9145-9160.
- Boebel, O., Duncombe Rae, C., Garzoli, S., Lutjeharms, J., Richardson, P., Rossby, T., Schmid, C., Zenk, W., 1997. Float experiment studies interocean exchanges at the tip of Africa. *Eos, Transactions of the American Geophysical Union* 79, 1, 7-8.
- Boebel, O., Anderson-Fontana, S., Schmid, C., Anson, I., Lazarevich, P., Lutjeharms, J., Prater, M., Rossby, T., Zenk, W., 2000. KAPEX RAFOS Float Data Report 1997- 1999. Part A: The Agulhas- and South Atlantic Current Components. GSO Technical Report 2000-2; UCT

- Oceanography Report 2000-1; Berichte aus dem Institut für Meereskunde an der Christian-Albrechts-Universität – Kiel, IFM 318, pp. 194.
- Boebel, O., Lutjeharms, J. R. E., Rossby, T. and Zenk, W., 2001a. The Cape Cauldron: an Agulhas mixing and exchange regime. *Deep-Sea Research*, this issue.
- Boebel, O., Rossby, T., Baron, A., Lutjeharms, J. R. E., Zenk, W., 2001b. Path and variability of the Agulhas Return Current. *Deep-Sea Research*, this issue.
- Bryan, K., 1969. A numerical method for the study of the circulation of the world ocean. *Journal Computational Physics* 4, 347-376.
- Byrne, D. A., Gordon, A. L., Haxby, W. F., 1995. Agulhas eddies: a synoptic view using Geosat ERM data. *Journal of Physical Oceanography* 25, 902-917.
- Cox, M. D., 1984. *A primitive equation, 3-dimensional model of the ocean*. GFDL Ocean Group technical report no. 1, Princeton University.
- De Ruijter, W. P. M., Biastoch, A., Drijfhout, S. S., Lutjeharms, J. R. E., Matano, R. P., Pichevin, T., van Leeuwen, P. J., Weijer, W., 1999. Indian-Atlantic inter-ocean exchange: dynamics, estimation and impact. *Journal of Geophysical Research* 104, 20,885-20,911.
- Duncombe Rae, C. M., Garzoli, S. L., Gordon, A. L., 1996. The eddy field of the South-East Atlantic Ocean: a statistical census from the BEST project. *Journal of Geophysical Research* 101, 11,949 – 11,964.
- Garzoli, S. L., Gordon, A. L., Kamenkovich, V., Pillsbury, D., Duncombe Rae, C., 1996. Variability and sources of the southeastern Atlantic circulation. *Journal of Marine Research* 54, 1039-1071.
- Garzoli, S. L., Goñi, G. J., Mariano, A. J., Olson, D. B., 1997. Monitoring the upper southeastern Atlantic transports using altimeter data. *Journal of Marine Research* 55, 453-481.
- Goni (sic), G. S., Garzoli, S. L., Roubicek, A., Olson, D., Brown, O., 1997. Agulhas ring dynamics from TOPEX/POSEIDON satellite altimeter data. *Journal of Marine Research* 55, 861-883.
- Gordon, A. L., 1985. Indian-Atlantic transfer of thermocline water at the Agulhas retroflection. *Science* 227, 1030-1033.
- Gordon, A. L., 1986. Inter-ocean exchange of thermocline water. *Journal of Geophysical Research* 91, 5037-5046.
- Gordon, A. L., Lutjeharms, J. R. E., Gründlingh, M. L., 1987. Stratification and circulation at the Agulhas Retroflection. *Deep-Sea Research* 34, 565-599.
- Gordon, A. L., Weis, R. F., Smethie, W. M., Warner, M. J., 1992. Thermocline and intermediate water communication between the South Atlantic and Indian Oceans. *Journal of Geophysical Research* 97, 7223-7240.
- Han, Y.-J., 1984. A numerical World Ocean general circulation model. Part II. A baroclinic experiment. *Dynamics of Atmosphere and Oceans*, 8, 141-172.
- Haney, R. L., 1971. Surface thermal boundary condition for ocean circulation models. *Journal of Physical Oceanography*, 1, 241-248.
- Harris, T. F. W., 1972: Sources of the Agulhas Current in the Spring of 1964. *Deep-Sea Research and Oceanographic Abstracts*, 19(9)
- Kraus, E. B., Turner, J. S., 1967. A one-dimensional model of the seasonal thermocline. II: The general theory and its consequences. *Tellus*, 19, 98-105.
- Levitus, S., Boyer, T., 1994. *NOAA Atlas NESDIS 4. World Ocean Atlas 1994. Vol. 4: Temperature*. U. S. Department of Commerce. National Oceanic and Atmospheric Administration, pp. 117.
- Levitus, S., Burgett, R., Boyer, T. P., 1994. *NOAA Atlas NESDIS 4. World Ocean Atlas 1994. Vol 3: Salinity*. U. S. Department of Commerce. National Oceanic and Atmospheric Administration, pp. 99.
- Lutjeharms, J. R. E., van Ballegooyen, R. C., 1988. The retroflection of the Agulhas Current. *Journal of Physical Oceanography* 18, 1570-1583
- Lutjeharms, J. R. E., Cooper, J., 1996. Interbasin leakage through Agulhas Current filaments. *Deep-Sea Research* 43, 213-238.
- Lutjeharms, J. R. E., 1996. The exchange of water between the South Indian and the South Atlantic. In *The South Atlantic: Present and Past Circulation*, editors: G. Wefer, W. H. Berger, G. Siedler and D. Webb, Springer-Verlag, Berlin, pp. 125-162.
- Lutjeharms, J. R. E., Boebel, O., Rossby, T., 1997. KAPEX: an international experiment to study deep water movement around southern Africa. *South African Journal of Science* 93, 377-381.
- Lutjeharms, J. R. E., de Ruijter, W. P. M., Ridderinkhof, H., van Aken, H., Veth, C., van Leeuwen, P. J., Drijfhout, S. S., Jansen, J. H. F., Brummer, G.-J. A., 2000. MARE and ACSEX:

- new research programmes on the Agulhas Current system. *South African Journal of Science* 96, 105-110.
- Lutjeharms, J. R. E., Anson, I. J., 2001. The Agulhas Return Current. *Journal of Marine Systems*, 30, 115-138.
- Lutjeharms, J. R. E., Boebel, O., Rossby, T., 2001a. Agulhas cyclones. *Deep-Sea Research*, this issue.
- Lutjeharms, J. R. E., Boebel, O., van der Vaart, P. C. F., de Ruijter, W. P. M., Rossby, T. H., Bryden, H. L., 2001b. Evidence that the Natal Pulse involves the Agulhas Current to its full depth. *Geophysical Research Letters* 28, 3449-3452.
- Maltrud, M.E., R. D. Smith, A. J. Semtner, R. C. Malone, 1998: Global eddy-resolving ocean simulations driven by 1985-1995 atmospheric winds. *Journal of Geophysical Research: Oceans*, 103, 30,825-30,853.
- Mason, S.J., 1995: Sea-surface temperature - South African rainfall associations, 1910-1989. *International Journal of Climatology*, 15, 119-135.
- Matano, R. P., Simionato, C. G., de Ruijter, W. P., van Leeuwen, P. J., Strub, P. T., Chelton, D. B., Schlax, M. G., 1998. Seasonal variability in the Agulhas retroflection region. *Geophysical Research Letters*, 25, 4361-4364
- Matano, R.P., Beier, E.J., Strub, P.T., 2001: Large-scale forcing of the Agulhas variability: the seasonal cycle. *Journal of Physical Oceanography*, in press.
- Pacanowski, R. C., 1996. MOM 2 version 2, documentation, user's guide and reference manual. Tech. Rep. 3.2, GFDL, 329 pp.
- Quartly, G.D., M.A. Srokosz, 1993: Seasonal variations in the region of the Agulhas retroflection: Studies with Geosat and FRAM. *Journal of Physical Oceanography*, 23, no. 9, 2107-2124.
- Reason, C.J.C., 1998: Warm and cold events in the southeast Atlantic /southwest Indian Ocean region and potential impacts on circulation and rainfall over southern Africa. *Meteorology and Atmospheric Physics*, 69, 49-65.
- Reason, C.J.C. and H.M. Mulenga, 1999: Relationships between South African rainfall and SST anomalies in the South West Indian Ocean. *International Journal of Climatology*, 19, 1651-1673.
- Ribbe, J., Tomczak, M., 1997. Effect of the missing Indonesian inflow in the Fine Resolution Antarctic Model. *Journal of Physical Oceanography*, 27, 445-455.
- Rouault, M., S.A. White, C.J.C. Reason and J.R.E. Lutjeharms, 2001: Evidence for the influence of the Agulhas Current on a South African extreme weather event. *Weather and Forecasting*, 17, 655-669.
- Schmid, C., Boebel, O., Zenk, W., Lutjeharms, J. R. E., Richardson, P., Garzoli, S., Barron, C., 2001. Early evolution of an Agulhas ring. *Deep-Sea Research*, 50, 141-166.
- Semtner Jr., A. J., Chervin, R. M., 1992. Ocean general circulation from a global eddy-resolving model. *Journal of Geophysical Research*, 97, 5493-5550.
- Stammer, D., Tokmakian, R., Semtner, A., Wunsch, C., 1996. How well does a 1/4° global ocean circulation model simulate large-scale oceanic observations? *Journal of Geophysical Research*, 101, 25779-25811.
- Stevens, D. P., 1990. On open boundary conditions for three dimensional primitive equation ocean circulation models. *Geophysical and Astrophysical Fluid dynamics*, 51, 103-133.
- Stramma, L., Lutjeharms, J. R. E., 1997. The flow field of the subtropical gyre of the south Indian Ocean. *Journal of Geophysical Research*, 102, 5513-5530.
- Thomson, S. R., Stevens, D. P., Döös, K., 1997. The importance of interocean exchange south of Africa in a numerical model. *Journal of Geophysical Research*, 102 (C2), 3303-3315.
- Valentine, H. R., Lutjeharms, J. R. E., Brundrit, G. B., 1993. The water masses and volumetry of the southern Agulhas Current region. *Deep-Sea Research* 40, 1285-1305.
- Van Ballegooyen, R. C., Gründlingh, M. L., Lutjeharms, J. R. E., 1994. Eddy fluxes of heat and salt from the southwest Indian Ocean into the southeast Atlantic Ocean: a case study. *Journal of Geophysical Research* 99, 14053-14070.
- Van Loon, H., Jenne, R.L., 1972: The zonal harmonic standing waves in the Southern Hemisphere. *Journal of Geophysical Research*, 77, 992-1003.
- Walker, N.D., 1990: Links between South African summer rainfall and temperature variability of the Agulhas and Benguela Current systems. *Journal of Geophysical Research*, 95, 3297-3319.
- Weijer, W., de Ruijter, W. P. M., Dijkstra, H. A., van Leeuwen, P. J., 1999. Impact of interbasin exchange on the Atlantic overturning circulation. *Journal of Physical Oceanography* 29, 2266-2284.
- Wunch, C., 1996: *The Ocean Circulation Inverse Problem*. Cambridge University Press.

Table 2.1 Depth averaged annual and seasonal mean volume fluxes (Sv) through different sections in the Agulhas Current region. Positive values refer to northward or eastward transport while negative values denote southward or westward transport.

Section	Lon and Lat	Annual	Summer	Autumn	Winter	Spring
A	35°S, 5-20°E	15.55	18.21	14.72	8.456	20.85
B	35°S, 20-35°E	-61.27	-57.58	-59.12	-63.63	-64.66
C	45°S, 5-20°E	12.93	14.29	12.92	10.6	13.96
D	45°S, 20-35°E	8.08	8.114	8.635	4.3	11.26
E	5°E, 35-45°S	-0.26	7.077	-0.729	-10.6	3.365
F	20°E, 35-45°S	-2.87	3.148	-2.523	-8.466	-3.535
G	35°E, 35-45°S	66.47	68.84	65.23	59.46	72.38
C	43°S, 5-20°E	11.25	16.99	15.16	7.12	5.855
C	47°S, 5-20°E	-5.2	-3.59	15.44	-8.62	-2.85
D	43°S, 20-35°E	8.7	9.22	4.911	5.126	15.50
D	47°S, 20-35°E	14.0	14.29	15.44	11.85	14.62
E	5°E, 35-43°S	-14.85	-10.39	-15.21	-24.72	-9.017
E	5°E, 35-47°S	13.20	20.00	12.36	2.937	17.65
F	20°E, 35-43°S	-19.15	-11.60	-14.76	-26.05	-24.01
F	20°E, 35-47°S	-7.558	-1.79	-8.112	-14.17	-6.054
G	35°E, 35-43°S	50.80	55.20	49.26	42.71	56.15
G	35°E, 35-47°S	67.74	70.08	66.44	61.30	73.23

Table 2.2 Annual mean volume fluxes (Sv) through different layers and sections in the Agulhas Current region.

Section	Lon and Lat	Total	0-436 m	436-1575 m	> 1575 m
A	35°S, 5-20°E	15.5	16.0	7.8	-8.3
B	35°S, 20-35°E	-61.3	-31.3	-28.1	-1.9
C	45°S, 5-20°E	12.9	6.7	6.8	-0.6
D	45°S, 20-35°E	8.1	3.9	3.6	0.6
E	5°E, 35-45°S	-0.3	11.0	-6.5	-4.8
F	20°E, 35-45°S	-6.4	1.1	-7.5	0
G	35°E, 35-45°S	66.5	34.8	26.9	4.8

Table 2.3 Depth averaged annual and seasonal mean heat fluxes (PW) through different sections in the Agulhas Current region. Positive values refer to northward or eastward transport while negative values denote southward or westward transport.

Section	Lon and Lat	Annual	Summer	Autumn	Winter	Spring
A	35°S, 5-20°E	1.03	0.92	1.10	0.97	1.11
B	35°S, 20-35°E	-2.93	-2.83	-2.79	-3.00	-3.08
C	45°S, 5-20°E	0.22	0.25	0.22	0.18	0.22
D	45°S, 20-35°E	0.14	0.16	0.15	0.10	0.16
E	5°E, 35-45°S	0.02	0.08	0.20	-0.16	-0.03
F	20°E, 35-45°S	-0.84	-0.66	-0.74	-1.00	-0.96
G	35°E, 35-45°S	2.25	2.33	2.20	2.11	2.35
C	43°S, 5-20°E	0.03	0.17	0.11	-0.08	-0.10
C	47°S, 5-20°E	0.15	0.19	0.15	0.11	0.17
D	43°S, 20-35°E	0.28	0.29	0.20	0.24	0.39
D	47°S, 20-35°E	0.21	0.23	0.22	0.18	0.23
E	5°E, 35-43°S	-0.212	-0.23	-0.06	-0.38	-0.20
E	5°E, 35-47°S	0.19	0.24	0.38	0.01	0.14
F	20°E, 35-43°S	-1.26	-1.05	-1.12	-1.40	-1.43
F	20°E, 35-47°S	-0.89	-0.72	-0.80	-1.04	-0.10
G	35°E, 35-43°S	1.90	2.02	1.86	1.72	2.013
G	35°E, 35-47°S	2.27	2.35	2.22	2.13	2.37

At 45°S There is a net surface heat loss of: Left box: -0.054 error:-0.0032
Right box: 0.015 error:0.001484

At 43°S There is a net surface heat loss of: Left box: -0.071 error:-0.032
Right box: -0.006 error:0.044

At 47°S There is a net surface heat loss of: Left box: -0.039 error:0.176
Right box: 0.035 error:0.0163

Table 2.4 Annual mean heat fluxes (PW) through different layers and sections in the Agulhas Current region.

Section	Lon and Lat	Total	0-436 m	436-1575 m	> 1575 m
A	35°S, 5-20°E	1.03	0.98	0.22	-0.17
B	35°S, 20-35°E	-2.92	-2.20	-0.86	0.14
C	45°S, 5-20°E	0.22	0.16	0.08	-0.02
D	45°S, 20-35°E	0.14	0.09	0.05	0
E	5°E, 35-45°S	0.02	0.23	-0.22	0.01
F	20°E, 35-45°S	-0.84	-0.68	-0.33	0.17
G	35°E, 35-45°S	2.25	1.56	0.72	-0.03

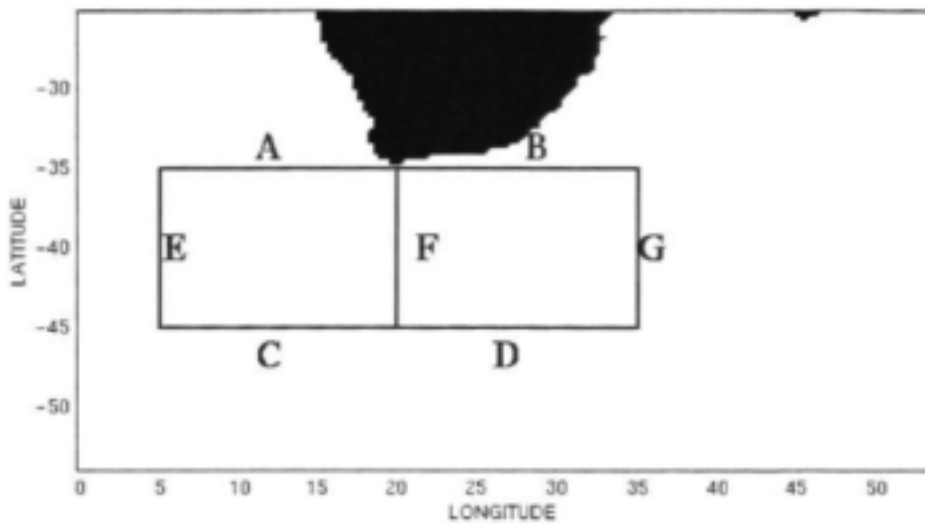


Figure 2.1 Schematic map showing transects in the southern Agulhas region through which high volume and heat transports have been calculated. After Reason et al. (2003).

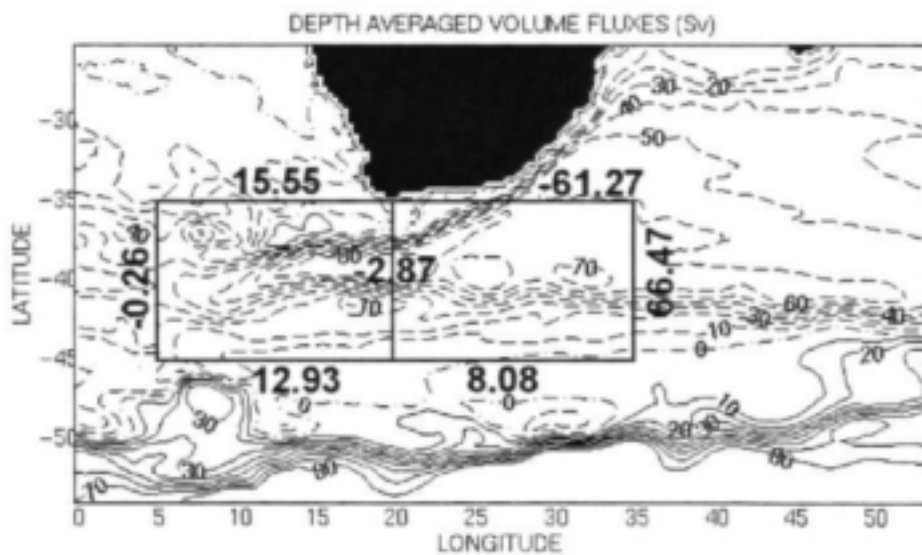


Figure 2.2 The annual mean total volume transport and barotropic streamfunction (Sv) averaged over years 31-35 of the model integration. After Reason et al. (2003).

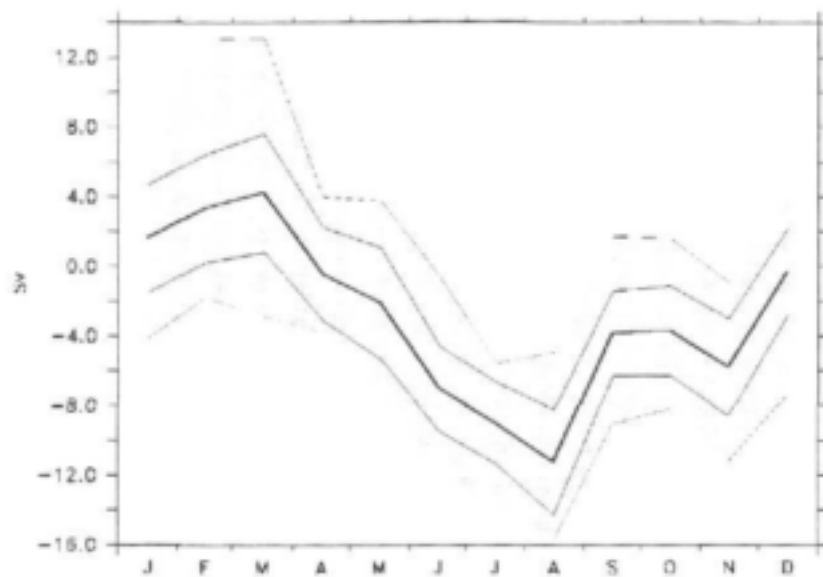


Figure 2.3a The monthly mean volume transport along 20°E between 45-35°S together with the maximum and minimum values and the standard deviation from the mean).

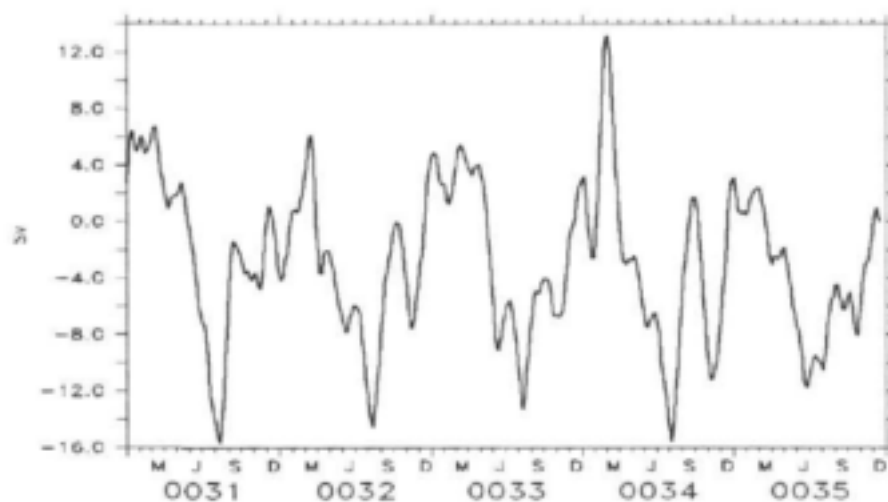


Figure 2.3b Time series of the volume transport along this section. After Reason et al. (2003).

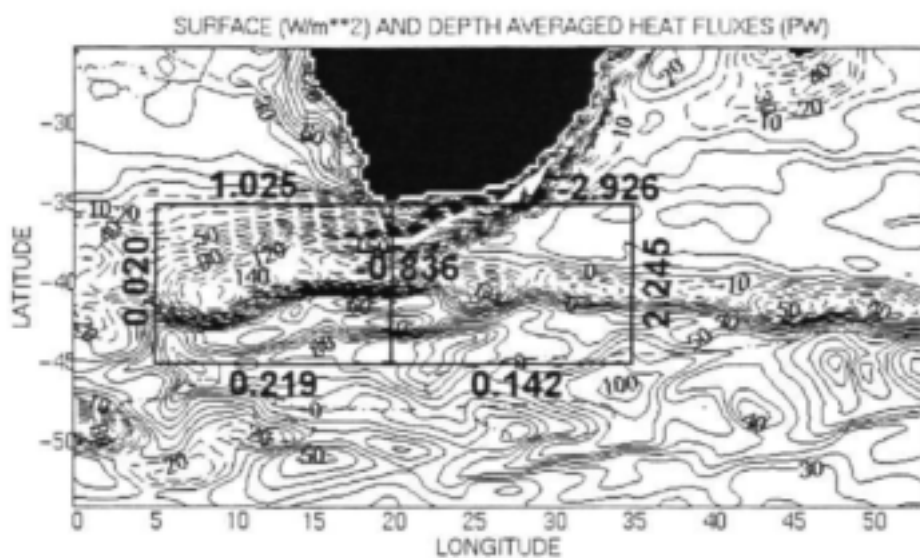


Figure 2.4 The annual mean total heat transport (PW) and net surface heat flux (Wm^{-2}) averaged over years 31-35 of the model integration. After Reason et al. (2003).

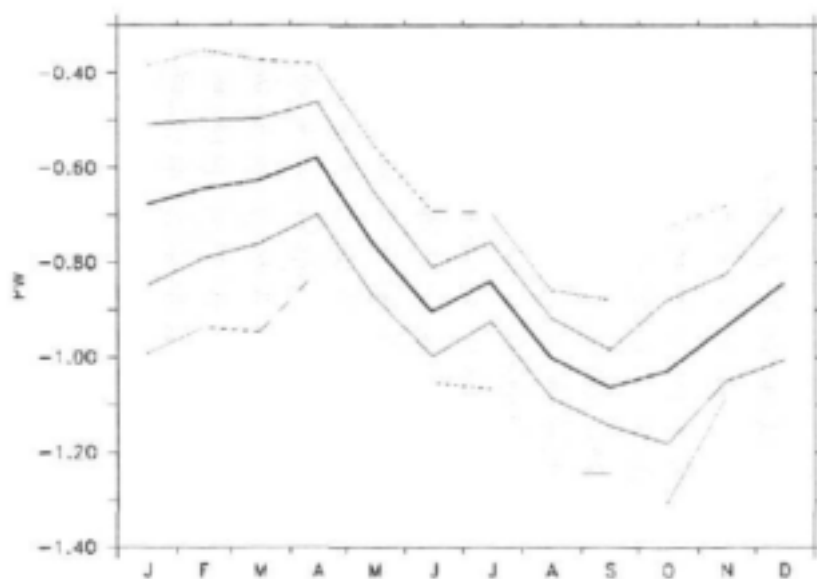


Figure 2.5a The monthly mean heat transport along 20°E between $45\text{-}35^{\circ}\text{S}$ together with the maximum and minimum values and the standard deviation from the mean.

Figure 2.5b Time series of the model heat transport along this section. After Reason et al. (2003).

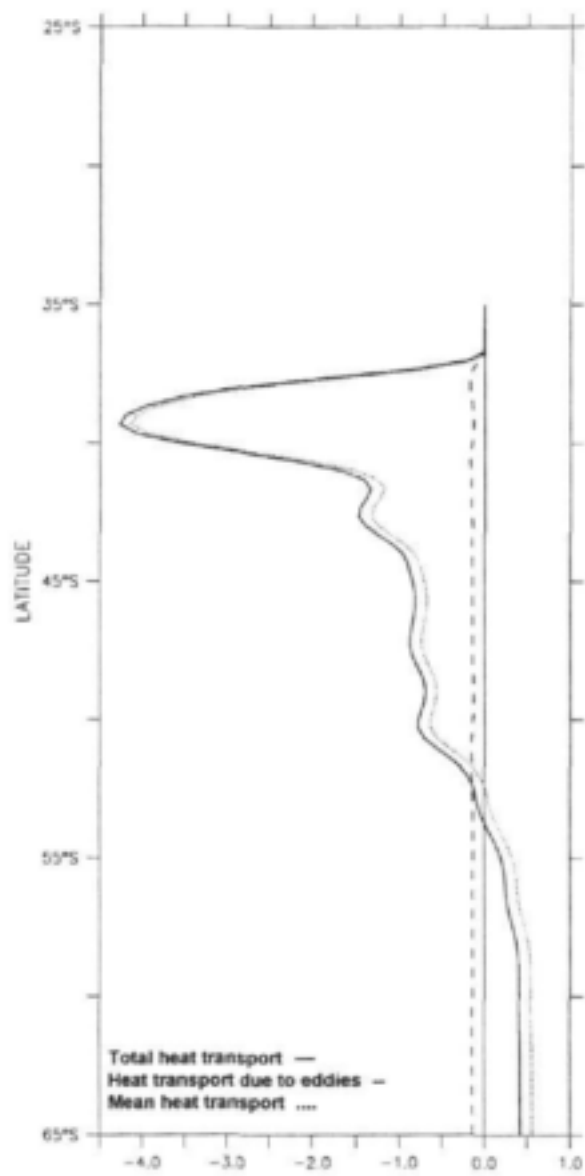
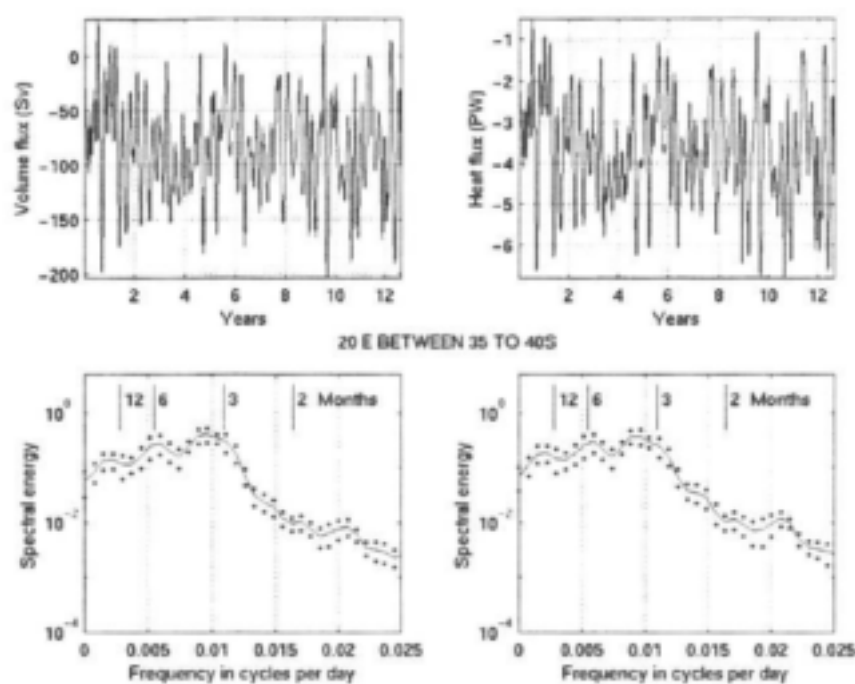


Figure 2.6 The total, mean and eddy heat transport at 20°E. After Reason *et. al* (2003).

A



B

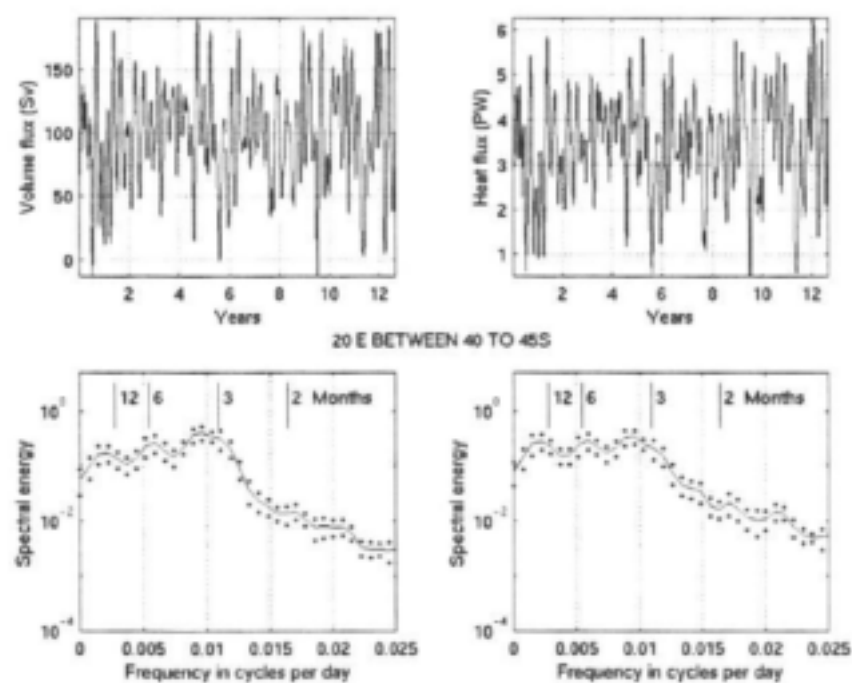
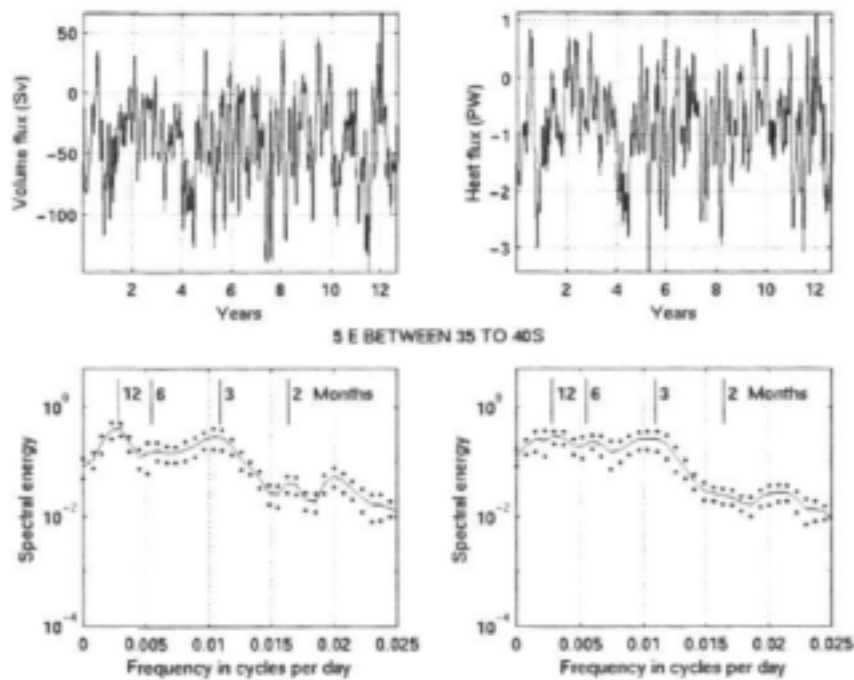


Figure 2.7 Time series and spectra of heat and volume fluxes from a 12 year integration of the model; (a) at 20°E between 35 to 40°S; (b) at 20°E between 40 and 45°S. After Reason et al. (2003).

A



B

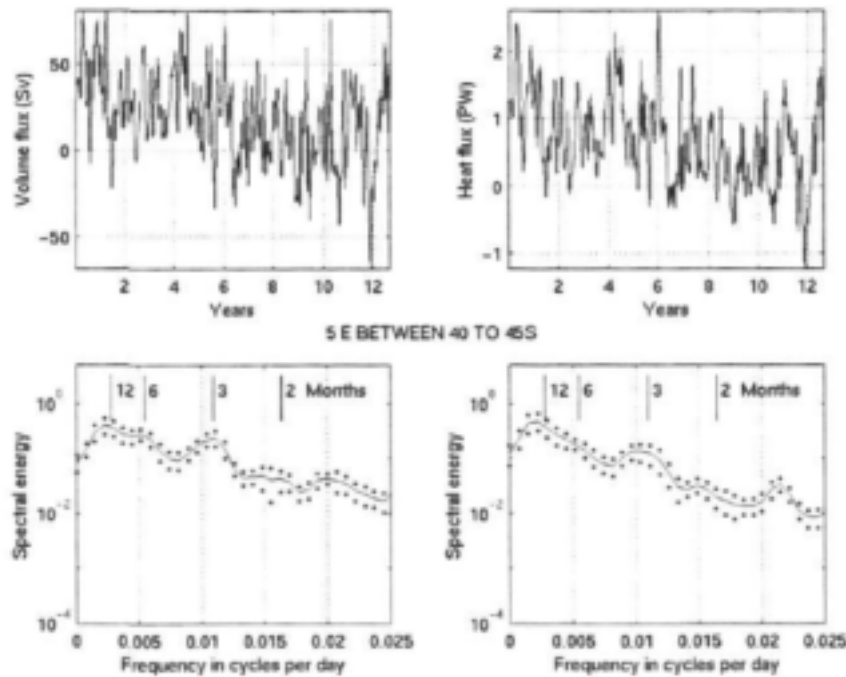


Figure 2.8 Time series and spectra of heat and volume fluxes from a 12 year integration of the model; (a) at 5°E between 35 to 40°S; (b) at 5°E between 40 and 45°S. After Reason et al. (2003)

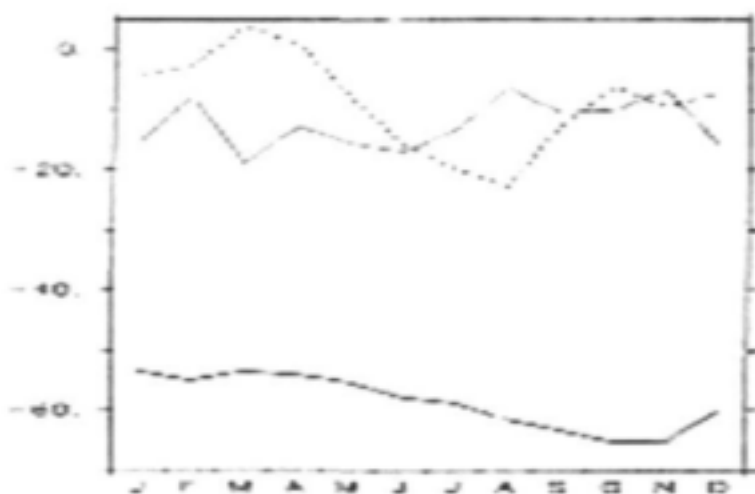


Figure 2.9 5-year climatology of the model transport of the Agulhas Current at 32°S (solid), through the Mozambique Channel at 23°S (dashed) and of the East Madagascar Current at 23°S (dotted); in Sv ($10^6 \text{ m}^3 \text{ s}^{-1}$). Note that flow south is negative. (After Biastoch *et al.*, 1999).

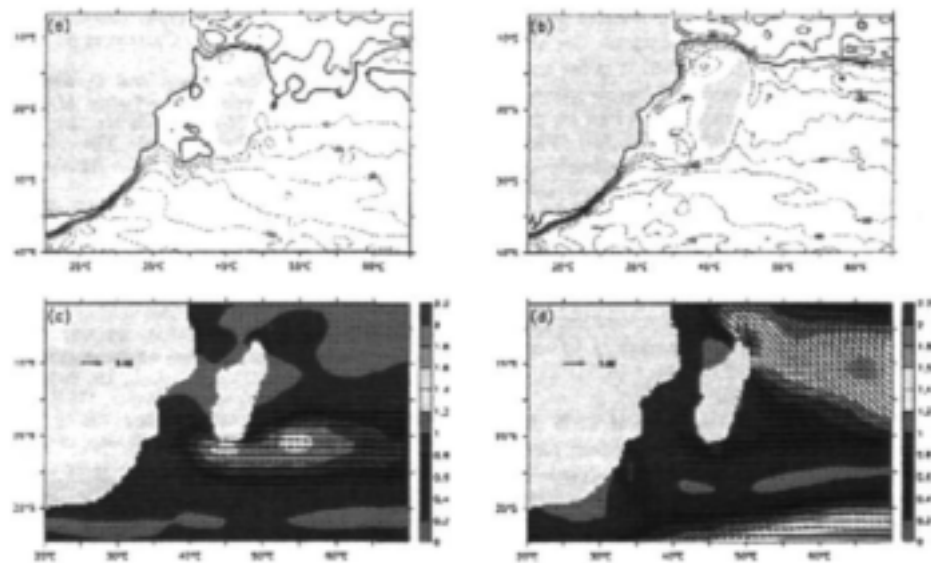


Figure 2.10 Stream function of the model transport in February (a) and August (b), in Sv. Absolute value and vectors of the wind stress in February (c) and August (d) (Note that only every third vector is drawn). Units are dynes cm^{-2} . (After Biastoch *et al.*, 1999).

3. Modelling the atmospheric response to an idealised SST anomaly in the South West Indian Ocean using a general circulation model

3.1 Introduction

Motivated by previous observational work (e.g., Walker, 1990, Mason, 1995) indicating strong statistical links between SST in the SW Indian Ocean and South African summer rainfall, various idealised AGCM experiments were carried out to investigate these links further and identify potential mechanisms. In all AGCM experiments described below, the Melbourne University AGCM was used. A brief description of the model follows.

In the horizontal, variables are represented in terms of spherical harmonics rhomboidally truncated at wave number 21. Prognostic variables are represented at 9 σ -levels. Envelope topography spectrally analysed from the $1^\circ \times 1^\circ$ topography data set of Gates and Nelson (1975) is used. Soil moisture content is computed from a two-layer scheme developed by Deardorff (1977) and surface fluxes are derived using Monin-Obukhov similarity theory as in Simmonds (1985). Precipitation in the model can be generated by the large-scale circulation whenever the relative humidity reaches 100%, and also through convective processes. Parameterization of the latter is via a modification (Weymouth, personal communication) of the moist convective adjustment scheme of Manabe *et al.*, (1965). The prescribed SST used in control integrations of the model is that of Reynolds (1988). As discussed by Simmonds *et al.* (1988), the model represents the current climate reasonably well and its performance is comparable with other GCMs of its type (e.g. Boer *et al.*, 1992). A number of climate sensitivity studies have been performed with the Melbourne University GCM, many to do with SST forcing in the tropics and related circulation and rainfall changes (e.g. Simmonds and Smith, 1986; Budd and Simmonds, 1990; Simmonds, 1990; Rocha and Simmonds, 1997).

Analyses of extratropical cyclone characteristics were conducted with the objective vortex finding and tracking scheme of Murray and Simmonds (1991a,b). To find depressions in the GCM integrations, the digital pressure fields on a conformal polar stereographic grid are represented in terms of continuous functions using cubic splines computed along the grid axes. An iterative differential routine based on ellipsoidal minimization techniques is used to define the location of lows in continuous space. Both closed (systems having a closed isobar at a given interval) and open depressions were included in the analysis. Locations of closed depressions were defined by minimization of the pressure functions, whereas open depressions, indicating inflections in the pressure field, were found by searching for minima in the absolute value of the local pressure gradient. To prevent the inclusion of small-scale or broad, shallow features associated with topography or other effects rather than genuine, migrating systems, a minimum curvature test (e.g. Jones and Simmonds, 1993) was applied. The ability of the Murray and Simmonds scheme to identify and track systems in the observational record has been demonstrated by Jones and Simmonds (1993), to whom the reader is referred for further details of the scheme's technical aspects and performance.

3.2 Experimental design

The model was forced with an idealized warm anomaly imposed on climatological (Reynolds, 1988) SST (fig.3.1). By choosing a smoothed idealization of the observed warming, it is hoped that the resulting atmospheric model response is that much more distinct and straightforward to diagnose. In order to take account of the inherent non-linearity of the atmosphere, results are derived from the mean of an ensemble of 11 integrations as in the method used by Reason *et al.* (1998). Each of these model integrations is forced by the same imposed SST anomaly but start from different initial conditions (i.e. different individual days from a previous extended control run of the model). The integrations each proceeded for approximately 2 years and the results shown below correspond to the austral autumn, spring and summer seasons of the year after initialization of each model run.

3.3 Precipitation and circulation changes over the adjacent landmasses

There are various changes in circulation and precipitation over the adjoining African landmass in response to the SST anomaly. Focus is mainly directed towards the seasons when southern Africa receives the bulk of its annual rainfall; thus, there is little interest in the austral winter in this context except for the southwestern margins of South Africa (winter rainfall maximum) or the south coast of South Africa (all seasons rainfall).

One may envisage that the imposed SST anomaly mainly east of South Africa (fig. 3.1) may result in both a local and a remote impact. Local modulations in the latent heat flux may result in changes to the amount of moisture advected onto the coastal region by prevailing southeasterly winds as well as in the intensity of any atmospheric disturbances passing over the anomaly. The latter can then influence tropical-temperate trough formation leading to rainfall changes over the landmass remote from the anomaly. Dynamical adjustment of the atmosphere to the anomaly (a warm region dynamically acts as negative orography, thereby potentially leading to a cyclonic anomaly; Gill, 1982) may contribute via modulations to the strengths of the prevailing winds and associated instability and moisture convergence over southern Africa.

Aspects of these modulations are evident in the model response to the warm SST anomaly. For example, model results suggest that the lower atmospheric response, particularly during the summer and autumn, is a cyclonic anomaly near, and downstream of, the SST forcing. This cyclonic anomaly not only represents a weakening of the subtropical high in the South Indian Ocean but is also favourable for tropical low formation over the southern African landmass. The latter appears particularly likely in summer where a cyclonic anomaly also exists at the 500 hPa level in the northern Namibia/southern Angolan region. Associated with the low level cyclonic anomaly over the Southwest Indian Ocean during each season, but particularly during the wetter summer and autumn months, is a southeasterly flow towards the South African east coast and westerly anomalies across tropical southern Africa (Figure 3.2). Upper level wind anomalies over tropical southern Africa tend to be easterly (Figure 3.3); this combination with the low level westerlies is thought to be associated with wet conditions over southern Africa since it implies convergence and ascent over the landmass (ascending branch of the local Walker circulation) with subsidence and low level divergence over the adjoining tropical South Indian and Atlantic Oceans.

The results of the extra-tropical cyclone tracking scheme applied to the model pressure fields indicated that there were increases in cyclone system density southeast of South Africa and in the intensity of these systems. The tracks tended to be further north suggesting, with the increases in density and intensity already noted, a significant midlatitude input into tropical-temperate troughs stretching NW-SE across South Africa. Thus, aspects of the model transient weather systems appear to respond in a way that also favours increased summer rainfall over eastern South Africa.

Both the marine southeasterly airstream and the tropical westerly anomalies are associated with moist airmasses, particularly the former (Figure 3.4). Thus, where there is enhanced convergence between these winds over southeastern Africa, one might expect increased convection and rainfall. Analysis of the model fields indicated that there were significant increases in relative convergence over northeastern South Africa, Mozambique and Zimbabwe during summer, and to lesser extent, autumn (not shown). Some areas of increased convergence over southern Africa also occurred during spring (not shown) but they were not statistically significant. All three seasons displayed increases in model velocity potential (not shown) over this southeastern region, implying relative ascent in the lower atmosphere which is favourable for increased rainfall. During summer, there were large regions of subsidence over the South Atlantic in the model (not shown), consistent with an ascending Walker limb over southern Africa and descending over the ocean areas to the

west. Consistent with these changes in circulation and the low level convergence of moist air masses (Figures 3.2–3.4), are significant positive rainfall anomalies over eastern South Africa and southern Mozambique during autumn, spring and summer (Figure 3.5).

Maximum rainfall increases tend to be near the coast with strong gradients inland near the Drakensberg mountains. This suggests that surface heating and moisture contrasts as well as orographic effects may play a role in locally enhancing the rainfall changes. During winter, weaker rainfall increases were noted (not shown) which were mainly confined to the south and southeast coasts of South Africa. This pattern is consistent with the climatology of this region which is one of all season rainfall, with that during winter being associated with cold fronts. Further north, the subtropical high is very dominant over the landmass during winter, and the model velocity potential anomalies for this season (not shown) imply relative subsidence, unfavourable for rainfall.

When accumulated over the given season, the magnitude of the rainfall increases over southeastern Africa are of the order 90–180 mm (autumn), 90–225 mm (spring), and 90–300 mm (summer). These represent a sizeable fraction of the mean seasonal totals further reinforcing the potential importance of SST anomalies in the Southwest Indian Ocean. However, further investigations with higher resolution models would be necessary before these model results can be regarded as more than suggestive. GCMs like that used here may have difficulties with simulating regional precipitation, particularly where this is influenced by local factors such as steep orography which cannot be represented by the relatively coarse resolution. Mesoscale numerical models offer an alternative to improve regional representation; however, their computational expense precludes integration on the seasonal to interannual timescales considered here. Downscaling techniques using some of the dynamical fields produced by the GCM to infer precipitation may be a practical alternative but this is beyond the scope of the current study.

Figures 3.2–3.5 have suggested that much of the increased rainfall over southeastern Africa arises from the convergence of moist airmasses that originate mainly over the tropical to subtropical South Indian Ocean. Examination of the mixing ratio, wind and latent heat flux anomalies (Figures 3.2, 3.4 and 3.6) suggests two somewhat related mechanisms behind the moister air advecting towards southeastern Africa. The first involves a local response, namely enhanced evaporation (Figure 3.6) of moisture off the warm SST anomaly by the prevailing southeasterlies (Figure 3.2). Combining with this locally-enhanced evaporation is the effect of the remote circulation anomalies induced by the SST forcing. These (Figure 3.2) show tropical westerly anomalies, originating over tropical southern Africa and the western equatorial Indian Ocean, extending well into the central subtropical South Indian Ocean and subsequently feeding into southeasterly anomalies east and southeast of South Africa.

The magnitude of the contribution of the locally-enhanced evaporation to the rainfall increases over adjacent southeastern Africa can be estimated by dividing the numbers in Figure 3.6 by 28.5 to convert from latent heat flux units of Wm^{-2} to mm/day (rate of evaporation or precipitation). This procedure leads to maximum values just off the coast of 2 mm/day (autumn), 1.9 mm/day (spring) and 2.8 mm/day (summer) which implies (cf. fig. 3.5) that most of the increased rainfall comes from locally increased evaporation off the warm SST anomaly. Some of the remaining rainfall increase appears to come from evapotranspiration off the coastal landmass (Figure 3.6 shows strong latent heat flux gradients extending to the Drakensberg mountains) with the remainder arising from convergence of moist airmasses that originate remote (tropical Africa, western equatorial Indian Ocean) from the SST anomaly.

3.4 Summary

The model results suggest that SST anomalies of the order 1-2°C over the southwest Indian Ocean result in quite significant seasonal rainfall changes over adjoining southeastern Africa. It should be noted that these imposed SST anomalies are comparable in magnitude to those observed during individual wet or dry seasons in the region. Accumulated over a given season, the model rainfall anomalies are about 90-300mm and, therefore, represent a sizeable fraction of the annual total in many areas.

The mechanism by which rainfall is modified in the model in response to the anomalous SST appears to involve changes in the convergence over southeastern Africa of moist air streams which originate from either the tropical south Indian Ocean or the tropical south Atlantic by way of low-latitude southern Africa. On the larger scale, there appear to be coherent low level westerly anomalies over tropical southern Africa and easterly anomalies aloft, a situation which has been previously identified in observational studies as being associated with increased rainfall over South Africa since it implies that the ascending branch of the local Walker circulation is located over the landmass with subsidence over the surrounding oceans. Thus the mechanisms by which model rainfall increases arise tend to be consistent with what might be expected observationally. The model results suggest that ongoing monitoring of SST in the southwest Indian Ocean is needed for improved understanding of South African rainfall variability.

The work presented above has provided evidence that an AGCM can be usefully applied towards investigating the sensitivity of South African seasonal rainfall and circulation patterns to SST anomalies in the SW Indian Ocean. However, each season is made up of a number of wet and dry spells and individual weather events. To understand these systems better, a mesoscale atmospheric model needs to be applied and the next section examines such an application to the extreme convective weather event that occurred over the southwestern and Eastern Cape during December 1998.

3.5 References

- Boer, G.J. et al., 1992: Some results from an intercomparison of the climates simulated by 14 atmospheric general circulation models. *J. Geophys. Res.*, 97, 12771-12786.
- Deardorff, J.W., 1977: A parameterization of ground-surface moisture content for use in atmospheric prediction models. *J. Appl. Meteor.*, 16, 1182-1185.
- Gates, W.L. and A.B. Nelson, 1975: A new (revised) tabulation of the Scripps topography on a 1 degree global grid. Part I: Terrain heights. The Rand Corporation, R-1276-1-ARPA, 132 pp.
- Harrison, M.S.J., 1984: A generalised classification of South African summer rain-bearing synoptic systems. *J. Climatology*, 4, 547-560.
- Jones, D.A. and I.H. Simmonds, 1993: A climatology of Southern Hemisphere extratropical cyclones. *Clim. Dyn.*, 9, 131-145.
- Mason, S.J., 1995: Sea-surface temperature - South African rainfall associations, 1910-1989. *Int. J. Climatology*, 15, 119-135.
- Murray, R.J. and I.H. Simmonds, 1991a: A numerical scheme for tracking cyclone centres from digital data. Part I: development and operation of the scheme. *Aust. Meteorol. Mag.*, 39, 155-166.
- Murray, R.J. and I.H. Simmonds, 1991b: A numerical scheme for tracking cyclone centres from digital data. Part II: application to January and July GCM simulations. *Aust. Meteorol. Mag.*, 39, 167-180.
- Reason, C.J.C., 1998: Warm and cold events in the southeast Atlantic / southwest Indian Ocean region and potential impacts on circulation and rainfall over southern Africa. *Met. Atmos. Phys.*, 69, 49-65.
- Reynolds, R.W., 1988: A real-time global sea surface temperature analysis. *J. Clim.*, 1, 75-86.
- Rocha, A. and I.H. Simmonds, 1997: Internannual variability of Southern African summer rainfall. Part II: Modelling the impact of sea surface temperatures on rainfall and circulation. *Int. J. Clim.*, 17, 267-290.
- Simmonds, I.H., 1985: Analysis of the 'spinup' of a general circulation model. *J. Geophys. Res.*, 90, 5637-5660.

- Simmonds, I.H., 1990: A modelling study of winter circulation and precipitation anomalies associated with Australian region ocean temperatures. *Aust. Meteorol. Mag.*, 38, 151-162.
- Simmonds, I.H. and I.N. Smith, 1986: The effect of the prescription of zonally-uniform sea surface temperatures in a general circulation model. *J. Climatology*, 6, 641-659.
- Simmonds, I.H. and A.H. Lynch, 1992: The influence of pre-existing soil moisture content on Australian winter climate. *Int. J. Clim.*, 12, 33-54.
- Simmonds, I.H., G. Trigg and R. Law, 1988: The climatology of the Melbourne University General Circulation Model. Publication No. 31, Meteorology, School of Earth Sciences, University of Melbourne., 67 pp. [NTIS PB 88 227491].

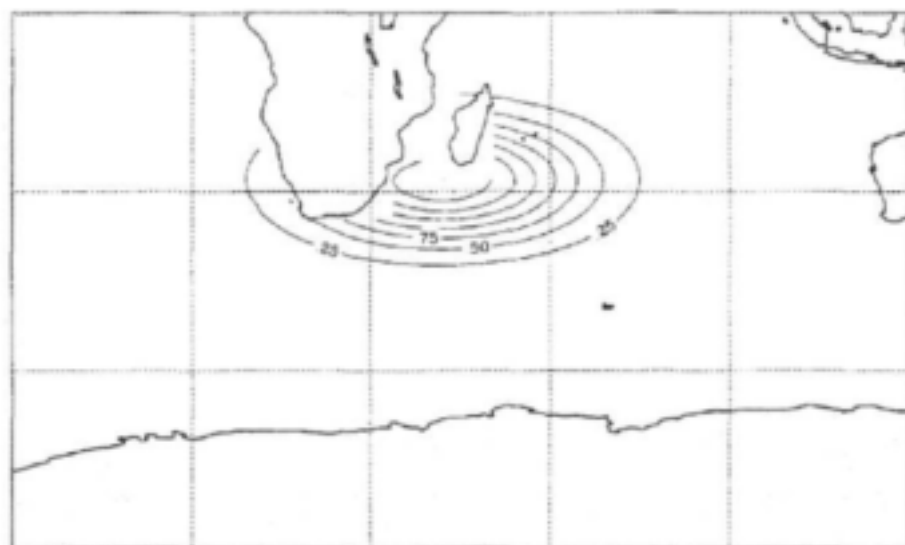
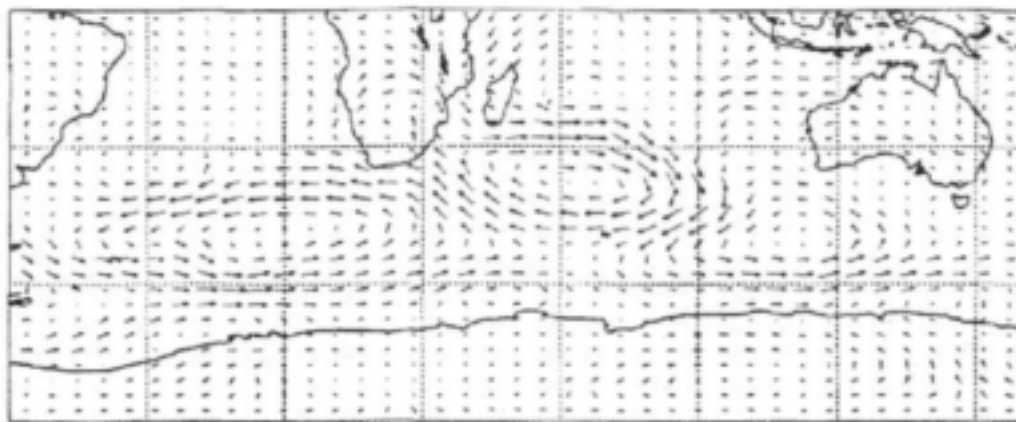
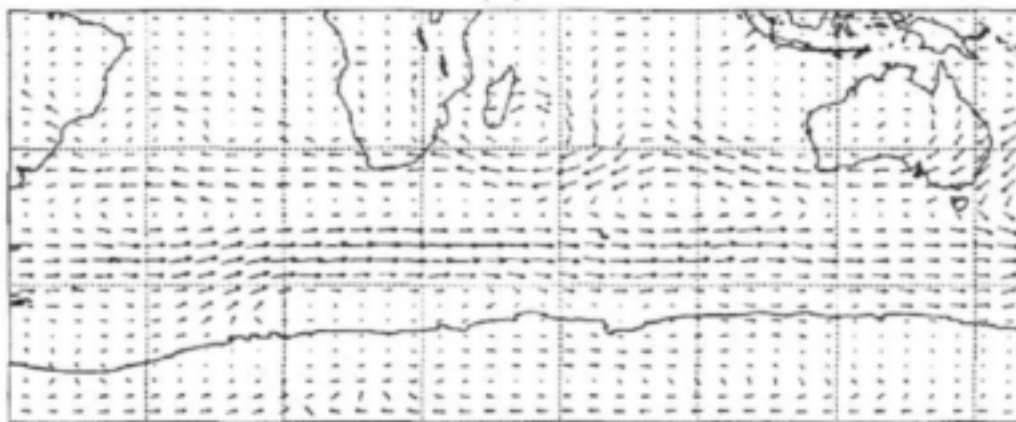


Figure 3.1 Idealization of the warming in the Southwest Indian Ocean imposed in the atmospheric model experiments. Contour interval 0.25°C



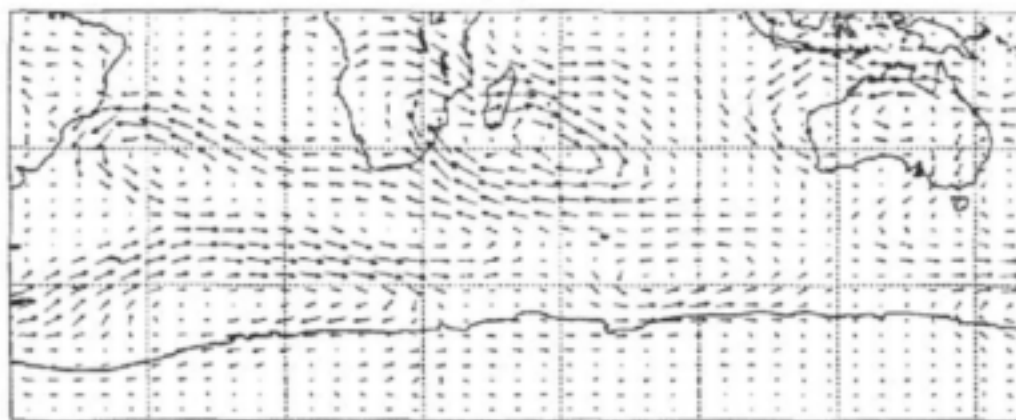
(a)

2.0 $\vec{m/s}$



(b)

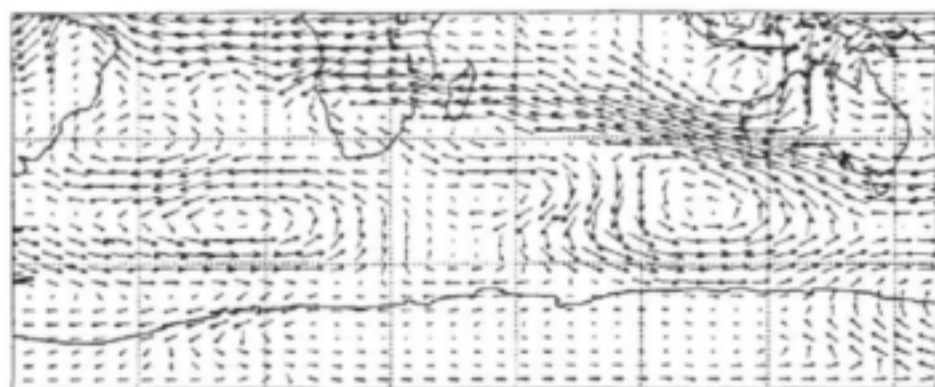
2.0 $\vec{m/s}$



(c)

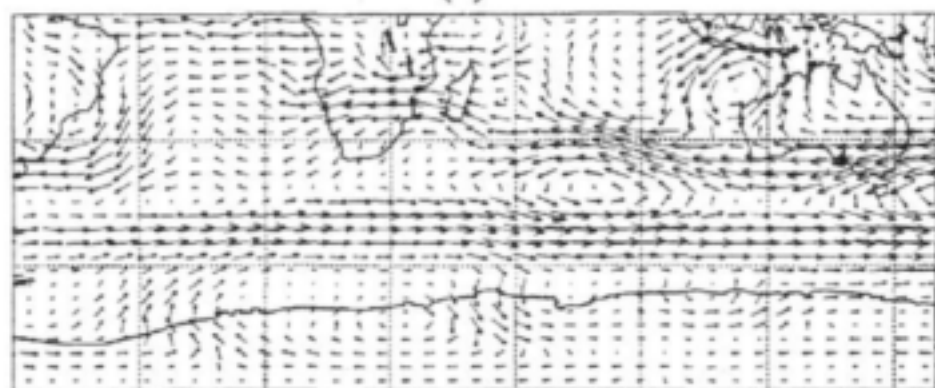
2.0 $\vec{m/s}$

Figure 3.2 Difference in winds at the 850 hPa level between the runs with the SST forcing and an ensemble of control runs for (a) austral autumn, (b) spring and (c) summer seasons. A scale vector is shown.



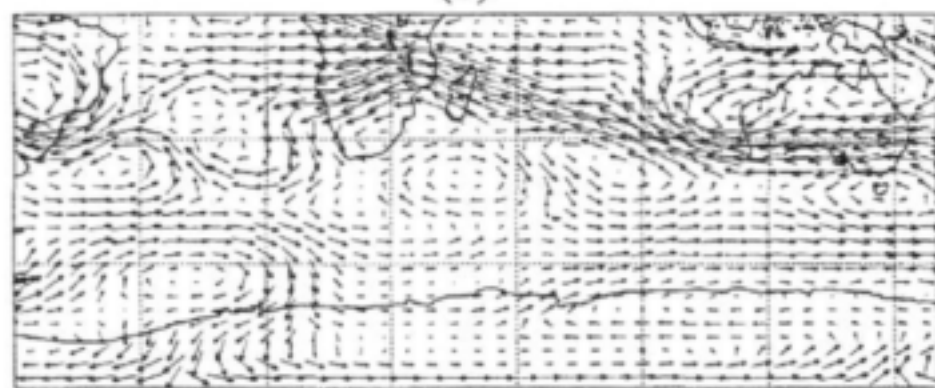
(a)

2.0 \vec{M}/S



(b)

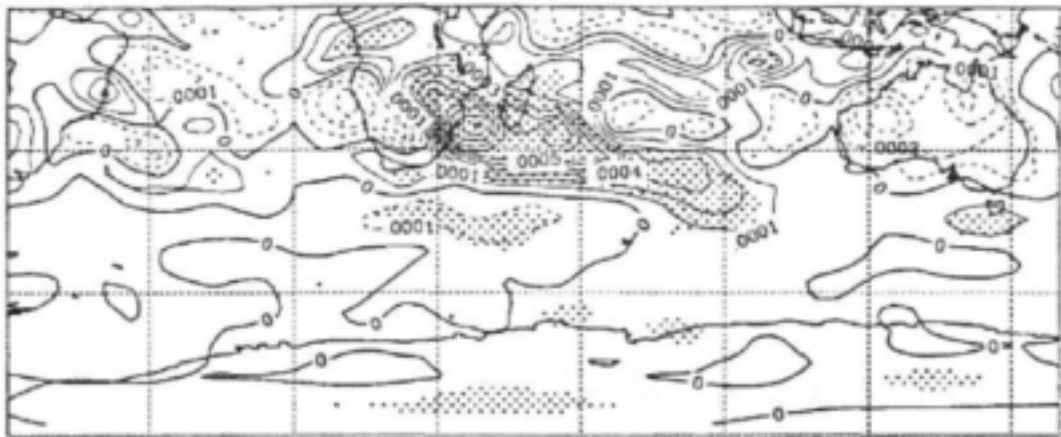
2.0 \vec{M}/S



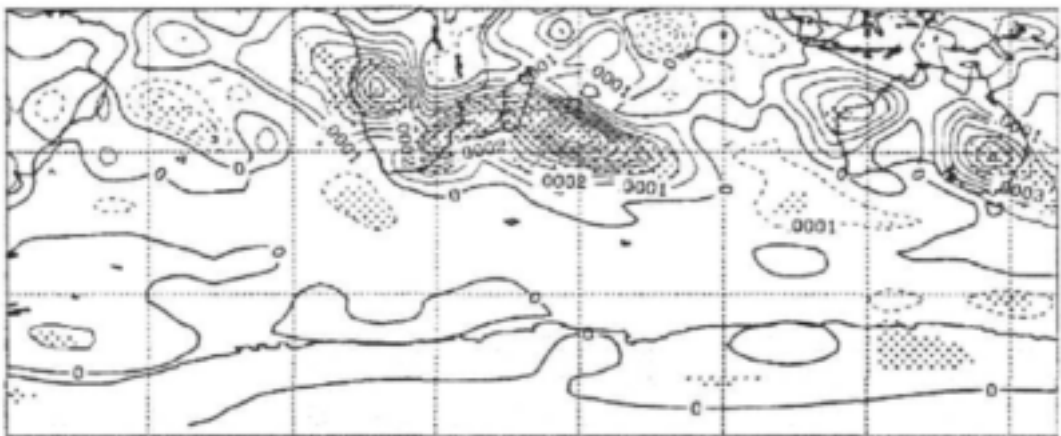
(c)

2.0 \vec{M}/S

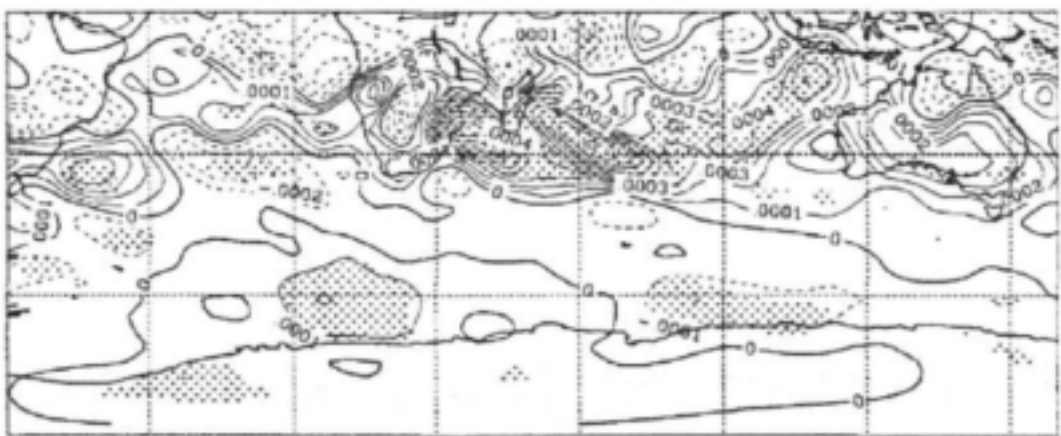
Figure 3.3 As for Fig. 3.2 except winds at the 200 hPa level.



(a)



(b)

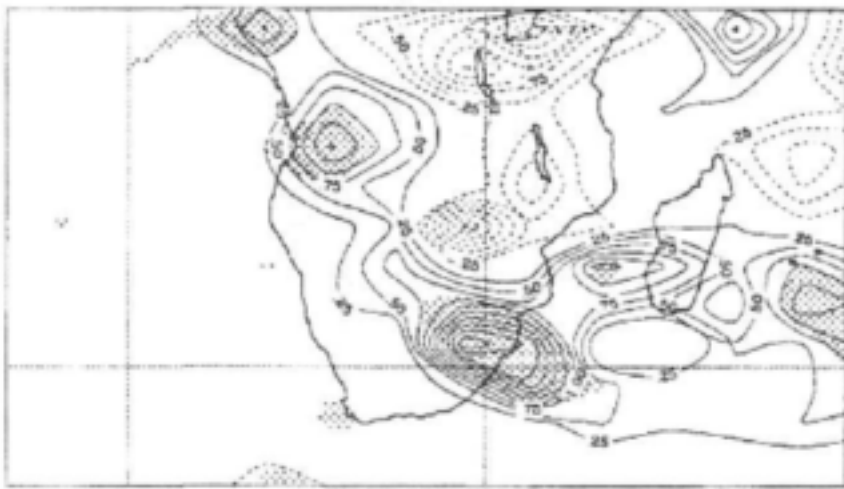


(c)

Figure 3.4 As for Fig. 3.2 except mixing ratio at the 850 hPa level. Contour interval 0.0001 kg/kg



(a)

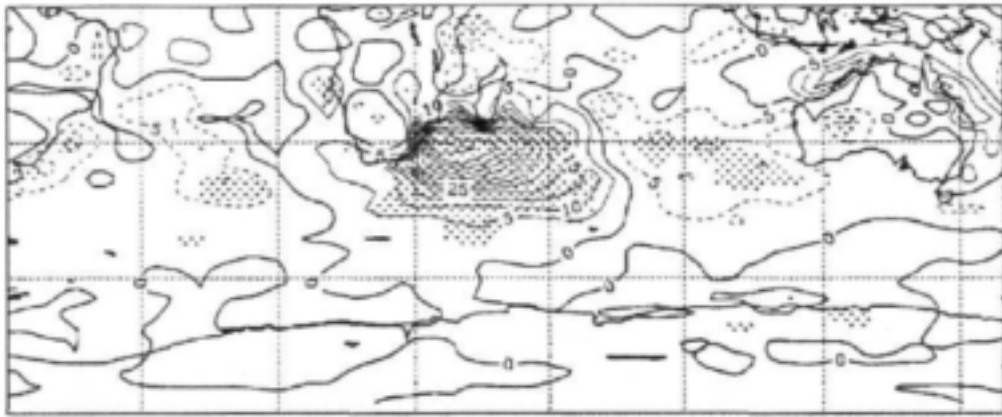


(b)

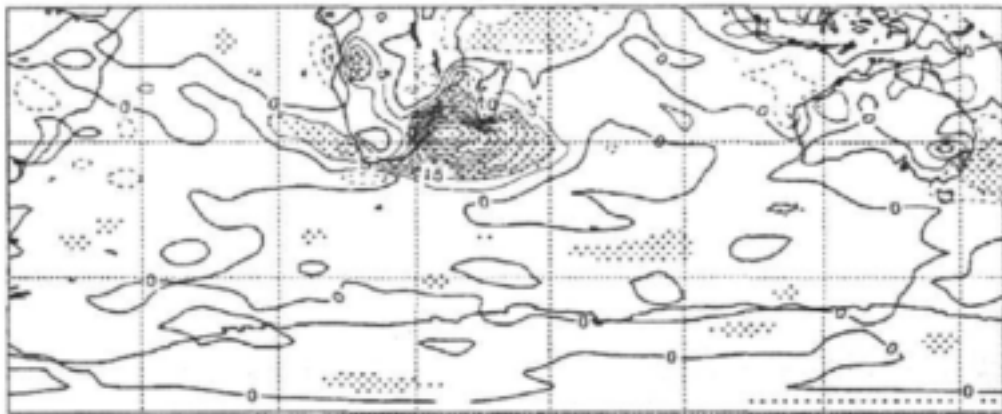


(c)

Figure 3.5 As for Fig. 3.2 except rainfall. Contour interval 0.25 mm/day



(a)



(b)

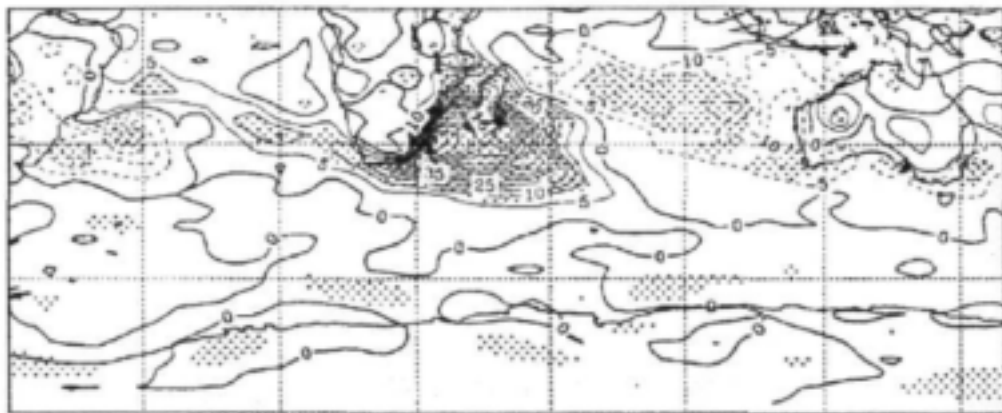


Figure 3.6 As for Fig. 3.2 except latent heat flux. Contour interval 5 Wm^{-2}

4. Using a regional atmospheric model to investigate moisture sources during the storm of December 1998

4.1 Introduction

Motivated by the observational analysis of the December 1998 storm (Rouault *et al.*, 2002 - henceforth referred to as RWRLJ02), a modelling study of the same storm was undertaken using a mesoscale atmospheric model. This mesoscale convective weather system produced flooding in the SW Cape on 14/12/98, and later evolved into extensive squall lines on 15/12/98 with significant rainfall in the Eastern Cape and tornado occurrence at Umtata and Hogsback. The objective was firstly to see whether a mesoscale model could capture the salient features of this devastating and complex weather system, and secondly, assuming this to be the case, to use the model to better understand the storm evolution and behaviour.

4.2 Model description and experiment design

MM5V3 is a limited-area, nonhydrostatic, terrain-following sigma-coordinate model designed to simulate or predict mesoscale and regional-scale atmospheric circulation. The model configuration includes a coarse mesh of 50km resolution, an intermediate mesh of 16.67km resolution and a fine mesh of 5.57km resolution (Fig. 4.1). Domain size for each mesh is 102x70, 181x121 and 337x145 respectively. There are 29 sigma levels in the vertical from the surface to 10 hPa. The model is initialised at 0000 UTC 10 December 1998 with data from NCEP reanalysis of 2.5°x2.5° resolution, which also provides the boundary conditions updated every 6 hours. Parameterisation of the model is summarised in table 4.1. Sea surface temperature (SST) data is taken from a combination of TRMM (Rouault *et al.*, 2001) and AVHRR satellite data, which is high resolution and resolves the temperature gradients and warm core of the Agulhas Current region accurately.

Table 4.1 MM5 options used

	Domain 1	Domain 2	Domain 3
Microphysics	Goddard	Goddard	Goddard
Cumulus	Grell	Grell	None
Boundary layer	MRF	MRF	MRF
Radiation	Cloud radiation	Cloud radiation	Cloud radiation

4.3 Weather station model validation

In this section, model performance is compared with weather station observations from the South African Weather Service (SAWS) on or near to the south coast of South Africa; namely, Cape Town, Port Elizabeth and East London. At all these stations, temperature is on the whole overestimated by the model, and surface pressure underestimated. A more detailed analysis from each of the weather stations follows.

Time series of temperature and surface pressure at the Cape Town International airport station are shown in figure 4.2. Observations show that on 13 December temperature reached a maximum of 31°C followed by a maximum of just 21°C on 14 December as heavy cloud developed over the region as can be seen from the satellite pictures in RWRLJ02 fig. 5. Over the following two days the diurnal cycle continues with a maximum temperature of 23°C on 15 December and 22°C on 16 December. The model underestimates maximum temperature on 13 December by about 3°C and overestimates by about 4°C on the following day. Moreover, the temperature trend on these two days is not well simulated by the model. Observations show that on 13 December temperature remains around 28°C for a prolonged period throughout the day whereas the model shows cooling

throughout the day after an early maximum. On 14 December, when heavy rainfall occurred over the Western Cape region, observations show that temperature remains cool around or just below 20°C throughout the day, whereas the model shows a typical diurnal cycle with warming in the morning followed by cooling in the afternoon. Outgoing longwave radiation from the model (fig. 4.9) shows that this warming is likely due to a lack of cloud over the region at this time. This may be due to the underestimation of temperature the previous day not generating enough convective uplift to form cloud. As will be seen later, the model heat low over the western interior is too far north and weak compared to observations and the midlevel westerly wave too weak. All these factors suggest insufficient instability and moisture content in the model airmass present over the Western Cape and therefore, compared to observations, less favourable conditions for convective cloud formation. On the following two days, the diurnal cycle is well simulated by the model, but with temperature overestimated by about 3°C on 15 December and about 1°C on 16 December.

Surface pressure in Cape Town shows a gradual increase of approximately 7 hPa from 13 – 16 December. Over the same time, the model shows a pressure increase of just 4 hPa. Throughout the period surface pressure is underestimated by the model, probably due to the overestimation of temperature. The trend of increasing pressure is well simulated except for a 2 hPa drop in model pressure early on 15 December. It is thought that this is due to the large overestimation of temperature on 14 and 15 December.

At the Port Elizabeth weather station (fig. 4.2) observations show temperature following a diurnal cycle with maximum temperature of about 25°C on 13 and 14 December. However, on 15 December, when the storm passes over the region (RWRLJ02 fig.5), there is no daytime increase in temperature with the maximum just over 20°C. On 13 and 14 December, the model follows the trend well, although temperature is overestimated by 2-3°C and leads observations in the morning and lags observations in the evening. On 15 December, the model continues to show daytime warming, with temperature overestimated by up to 9°C. Outgoing longwave radiation from the model (fig. 4.9) shows that there is some cloud over the region at this time, but not as thick as shown in the satellite pictures (RWRLJ02 fig. 5). Whether such a large overestimation of temperature can solely be attributed to a lack of cloud cover is debatable and there may be other factors influencing this (see section 6).

Observations of surface pressure in Port Elizabeth show a 9 hPa fall over the course of 13 December. The model initially underestimates the pressure by about 5 hPa, but over the same time period model pressure drops by just 5 hPa. Observations show that pressure begins to increase again from about midday on 15 December, but, probably due to the large overestimation of temperature on 15 December, model pressure does not begin to increase until early on 16 December, and is consequently underestimated by up to 6 hPa as the pressure increases.

At East London (fig. 4.2), the model appears to perform better than at the other locations. Observations show a clear diurnal cycle throughout the 13 – 16 December period, with lower daytime temperatures on the 15 and 16 December. The model follows this diurnal cycle well although temperature is generally overestimated by approximately 2°C.

Surface pressure is underestimated by the model by up to 10 hPa, and the initial drop in pressure is not so strong in the model. Similar to the case in Port Elizabeth, the final increase in pressure from the model lags observations by about 12 hours.

Overall, the model appears to overestimate temperature and underestimate pressure at the three coastal stations. The model generates insufficient cloud for already reasons mentioned briefly above and considered in more detail below, and this lack of cloud leads to

increased solar radiation at these stations and an overestimation of temperature during the period.

4.4 Sea level pressure and geopotential height

Mean sea level pressure synoptic charts from SAWS (RWRLJ02 fig. 4) show a heat low over the Western Cape of South Africa on 13 December which propagates east and deepens over the following two days before moving out to sea on 16 December. A well developed anticyclone is present over the south west Indian Ocean and there is a weak cold front to the south of South Africa. RWRLJ02 suggests that it is the interaction of this heat low, the trailing edge of the anticyclone and a midlevel westerly trough that was responsible for the storm.

Figure 4.3 shows model sea level pressure from 13 – 16 December. There is a well developed trough over southern Namibia and the Northern Cape but less evidence of a distinct heat low over the Western Cape as analysed in the SAWS synoptic charts. However, the depression over the SW Indian Ocean analysed in the synoptic chart on December 16 is captured by the model. The anticyclone in the South West Indian Ocean appears to be well simulated, but there is less evidence of the cold front, although the model domain may not extend far enough south for it to be seen.

However, due to the complex topography of South Africa, it is perhaps to be expected that these features will not be strongly apparent in the model sea level pressure fields. Figures 4.4–4.5 show the 850 hPa and 500 hPa geopotential height from 13 – 16 December. At 850 hPa, the heat low over the interior can be clearly seen on 13, 14 and 15 December, and the depression off the south east coast is well simulated on 16 December. The low over the interior is seen to deepen over the period 13 – 15 December from 1490 dam to 1480 dam. However, the eastward propagation of this feature suggested by the SAWS synoptic charts is not seen at this level in the model with the low remaining centred around 22°E from 13 – 15 December. At 700 hPa (not shown), there is little evidence of the thermal low apparent at 850 hPa consistent with it being a low level feature, forced by strong surface heating.

In order to investigate the reasons why the depression does not propagate east in the model, the *u* component of wind at 500 hPa and 200 hPa was examined and compared to NCEP. Figure 4.6 shows the difference between the *u* component of wind from the model and NCEP at 500 hPa. Over the central and western interior, it is clear that westerly component of the wind is much weaker in the model on 14 and 15 December by up to 8 m.s⁻¹. The cause of this large model discrepancy is still under investigation. Unlike observations, it appears that the westerly component of wind at 500 hPa is not strong enough to promote eastward advection of the low in the model. Similarly at 200 hPa (not shown), the westerly component of wind in the model is weaker than NCEP over the interior.

NCEP reanalysis data shows the presence of a midlevel trough propagating east over South Africa (RWRLJ02 fig. 6), which was thought to play an important role in the storm development. Figure 4.5 shows the model geopotential height at 500 hPa from 13 – 16 December. At 500 hPa, the trough is seen to be propagating eastwards over South Africa with time. However, on 15 December the trough does not appear to be as well pronounced in the model and, consistent with the too weak midlevel westerly winds in the model, its axis is located west of that resolved by NCEP. This discrepancy suggests that the model wave development is less marked than observed due to weaker temperature gradients and a less baroclinic model atmosphere

4.5 Moisture sources

RWRLJ02 concluded that the Agulhas Current and its recirculation in the south west Indian Ocean (henceforth Agulhas Current region) was a major source of low level moisture contributing to the storm. Analyses of moisture fluxes derived from wind and specific humidity data showed that at low levels there was a sizable flux of moisture onto the south coast of South Africa from the Agulhas Current region. A similar analysis was performed on the model output. Daily moisture flux values at the 1000, 850 and 500 hPa levels are shown in figure 4.7. At 1000 hPa, it can be seen that about $180 \text{ g.kg}^{-1} \text{ m.s}^{-1}$ of moisture was advected into the storm region on 13, 14 and 15 December; about $40 \text{ g.kg}^{-1} \text{ m.s}^{-1}$ more than suggested by NCEP. The model also shows that the moisture flux is much higher nearer to the coast of South Africa. This is due to the low resolution of the NCEP data, and potentially due to the NCEP model underestimating latent heat fluxes due to the low resolution of the SST data used not capturing the strong temperature gradients over the Agulhas Current (Rouault *et al.*, 2002). The moisture is advected by the easterly and northeasterly winds of the trailing edge of the anticyclone situated in the south west Indian Ocean (fig. 4.4). At 850 hPa, less moisture is advected into the storm region although motion is still anticyclonic over the south west Indian Ocean. This suggests that it is the moisture at the surface that is contributing most to the storm region.

At 700 hPa, up to $50 \text{ g.kg}^{-1} \text{ m.s}^{-1}$ is advected into the storm region from the north and west, consistent with NCEP, and at 500 hPa much drier air is advected into the region by the westerly wave discussed in section 4. The vertical wind shear, together with warm moist air at low levels and cool dry in the mid to upper levels are consistent with conditions favourable for severe storm and tornado formation.

Figure 4.8 shows latitudinal cross sections of moisture flux from 13 – 16 December at 35, 33 and 30°S. 35°S being the ocean just south of South Africa, 33°S across southern South Africa just inland of the coast, and 30°S the South African interior. RWRLJ02 performed latitudinal transects of moisture flux at 35° and 30°S and showed that there was a northward flux of low level moisture from the Agulhas Current whose maximum shifted east as the storm evolved. Maximum contribution to the storm of low level moisture from the Agulhas Current region occurred on 15 December. However the low resolution of the NCEP data does not give a clear indication of where the majority of the moisture is advecting. For example RWRLJ02 shows that between about 10°E and 20°E there is a northward flux of up to $80 \text{ g.kg}^{-1} \text{ m.s}^{-1}$ at 30°S. However the model suggests that there is a large northward flux of moisture over the south east Atlantic ocean west of 17°E, and a considerably smaller northward flux of about $30 \text{ g.kg}^{-1} \text{ m.s}^{-1}$ over the continent. NCEP also suggests that there is a greater northward flux at 30°S than at 35°S, whereas the model suggests the opposite. Inclusion of the 33°S latitudinal transect shows that as the air mass is advected northward from the ocean, the moisture content decreases consistent with significant precipitation over the southern Cape and coastal ocean.

The NCEP data also shows that the boundary between the northward moisture flux and southward moisture flux shifts to the east over the period of the storm. Figure 4.8 shows that at 30°S this boundary also moves to the east between 13 and 15 December and further still as the wind becomes southwesterly on 16 December. There is some eastward propagation of the boundary at 33°S, moving from around 27°E on 13 December to around 28°E on 15 December. However the boundary between the northward and southward moisture flux is wide as there is a large area of zero meridional flux. This may be due to the stationary nature of the thermal low in the model (fig. 4.4), which synoptic charts suggests propagates eastward over the period of the storm.

The model confirms that a large amount of moisture is advected into the storm region from the Agulhas Current region. However, latitudinal transects suggest that less moisture is advected from this region onto the continent than had previously been surmised from analy-

sis of NCEP data. Also since the model shows that the boundary between northward and southward flux of moisture is wide, the model may not be producing sufficient horizontal shear in the atmosphere to enhance vertical vorticity and therefore upward motion of the system.

4.6 Discussion and concluding remarks

Analysis of MM5 output has confirmed that the Agulhas Current region was a major source of low level moisture feeding the storm as concluded in RWRLJ02. However, MM5 is seen to have some weaknesses in simulating this event. In both Cape Town and Port Elizabeth temperature was greatly overestimated as the storm passed over these regions. Figure 4.9 shows outgoing longwave radiation (OLR) from the model at 2 hour intervals from 1000UTC 14 December to 1800UTC 15 December. It shows that convection produced by the model is not as organised as that seen from satellite pictures (RWRLJ02 fig. 5) with no initial circular convection and no discernable squall line. OLR from the model suggests that the reason that temperature has been greatly overestimated in Cape Town and Port Elizabeth is that the model is not producing enough cloud in these places at these times. There are a number of possible reasons for this weakness: weaknesses in the subgridscale schemes used by the model, inaccurate topography, inaccurate vegetation data, and the resolution of the forcing data.

Extensive testing of various parameterisations available in MM5 (not shown) has led us to believe that the chosen schemes perform best in simulating this event. It is possible that the available parameterisations, which were developed in the Northern Hemisphere, need to be significantly modified for South African conditions.

Topography used in the model is at 2 minute resolution for domain 3 shown in Fig. 4.1. Although land features seem to be fairly well resolved, many of the small scale topographical features are missing. Also around Cape Town the height of large features is greatly underestimated, e.g. Table Mountain which is around 1000m high is just 600m high in the model. Increasing the resolution of the topography in Cape Town and Port Elizabeth to 30 seconds and running the model with a fourth domain at higher resolution yielded little improvement in the time series at these stations.

The vegetation data used is from USGS, and it may be the case that this is not so applicable to South African vegetation. Initial conditions and boundary forcing is from the 2.5° x 2.5° NCEP reanalysis data, and it is possible that this forcing is not of sufficient resolution to properly simulate this event. We plan to run the model with higher resolution data from MRF in the future to assess sensitivity to higher resolution boundary and initial conditions. Ongoing work is applying the model to other storms; namely, the cut off low events of August 2002 and March 2003 that led to severe flooding in East London and Montagu respectively. A major problem in trying to simulate strongly convective storms of this nature is the lack of high resolution sounding data with which to initialise the model. Without high vertical resolution of initial temperature, moisture and winds, it is difficult for the model convective boundary layer to grow properly and to form sufficient convective cloud. This problem is likely to get worse for South African applications given the ongoing reduction in radiosonde releases.

4.7 References

- Rouault, M., S.A. White, C.J.C. Reason, J.R.E. Lutjeharms and I. Jobard, 2002: Ocean-Atmosphere Interaction in the Agulhas Current and a South African extreme weather event. *Weather and Forecasting*, **17**, 655-669.
- Rouault, M., C.J.C. Reason, J.R.E. Lutjeharms and A. Beljaars, 2003: Underestimation of latent and sensible heat fluxes above the Agulhas Current in NCEP and ECMWF analyses. *J. Clim.*, **16**, 776-782.

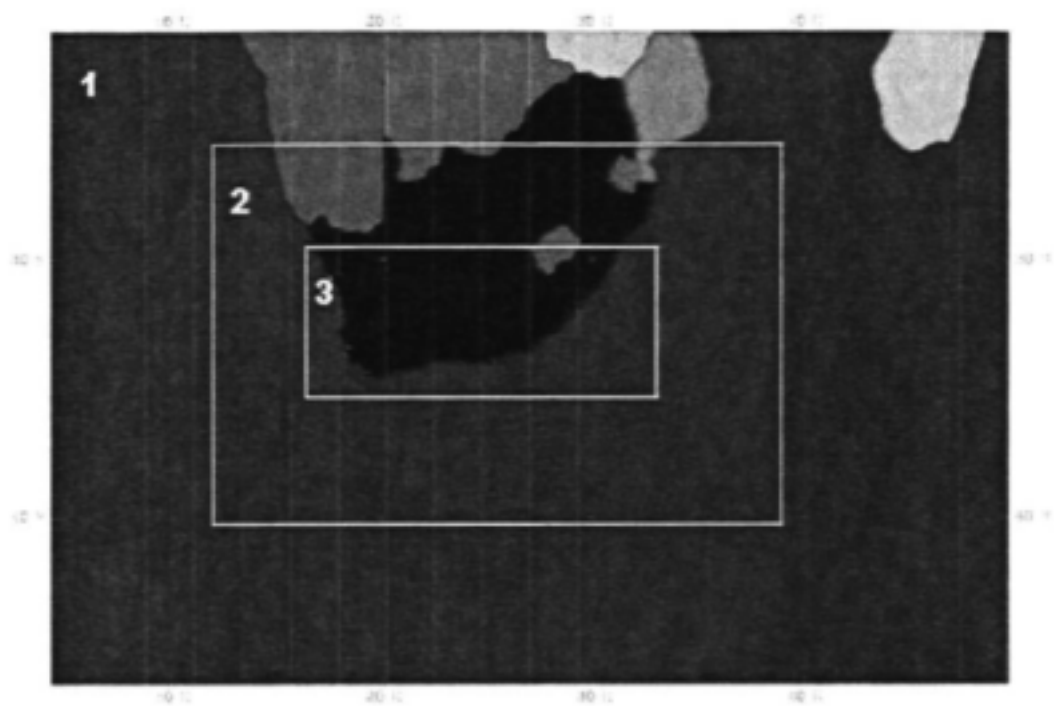


Figure 4.1 Model Domains

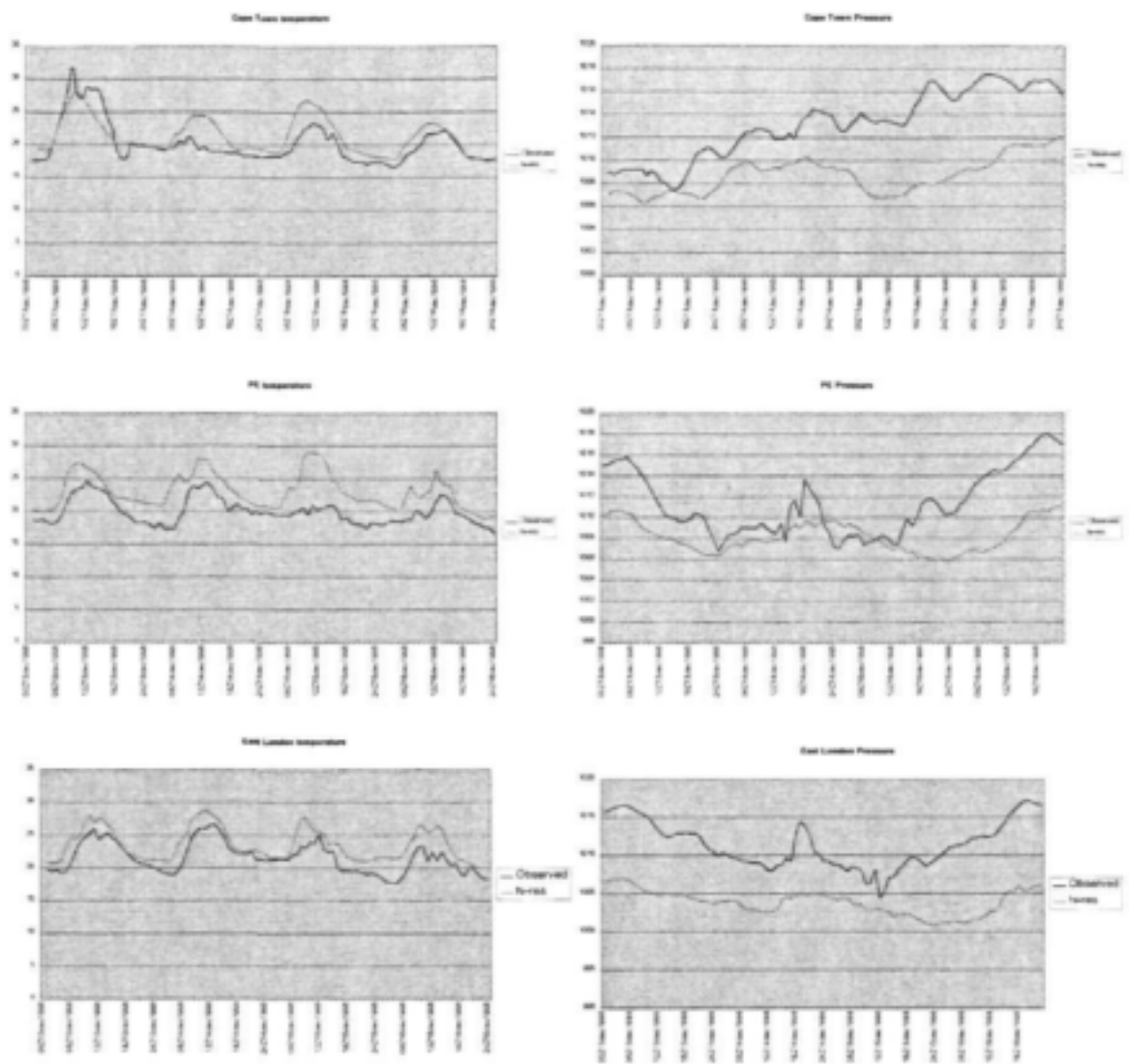


Figure 4.2 Time series of temperature and pressure in Cape Town, Port Elizabeth and East London. The blue line is the observed and the pink line the model output.

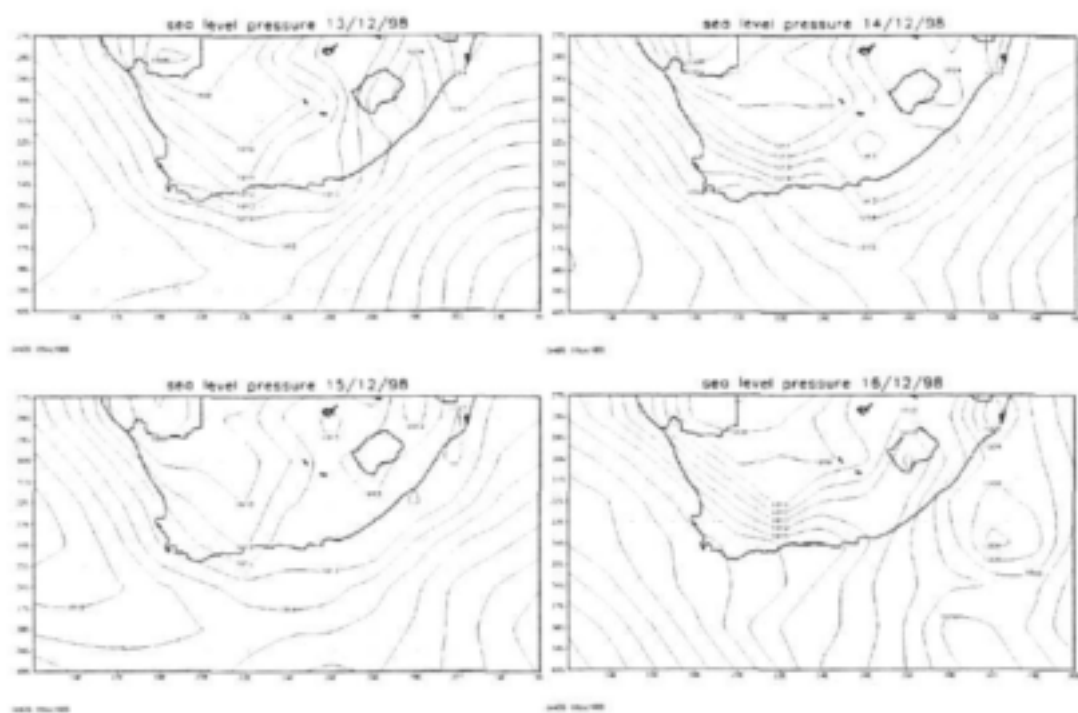
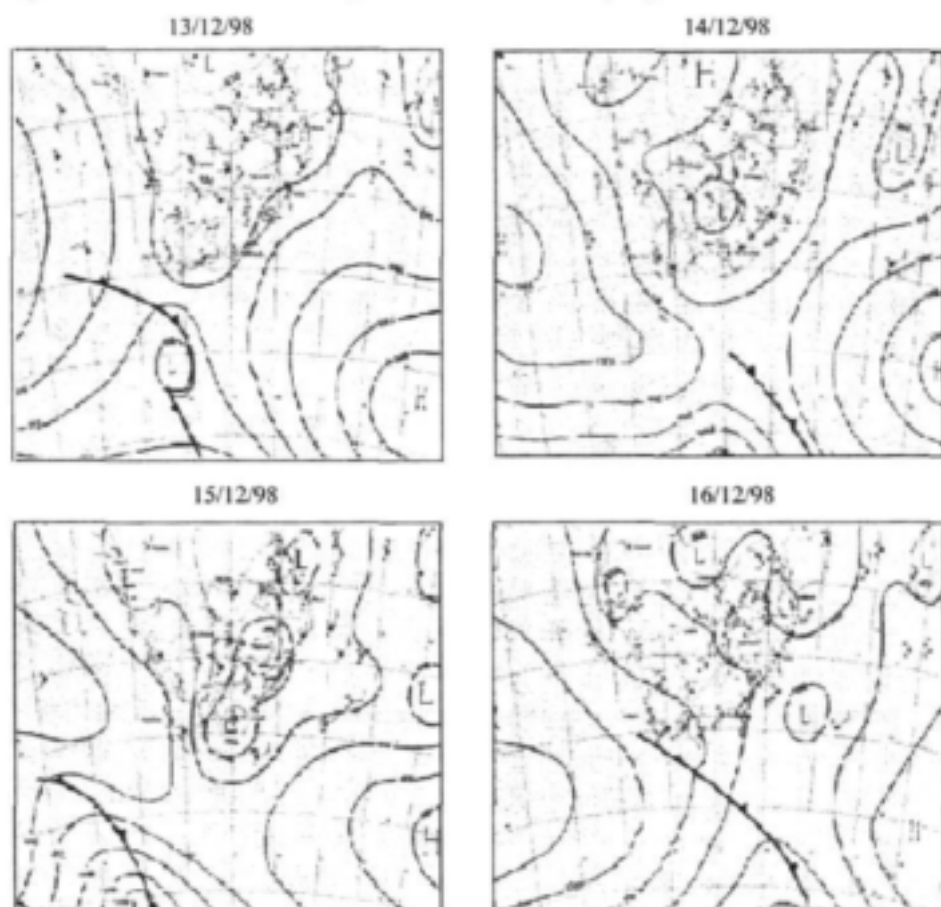


Figure 4.3 – Model sea level pressure and SAWS synoptic charts 13-16 December 1998



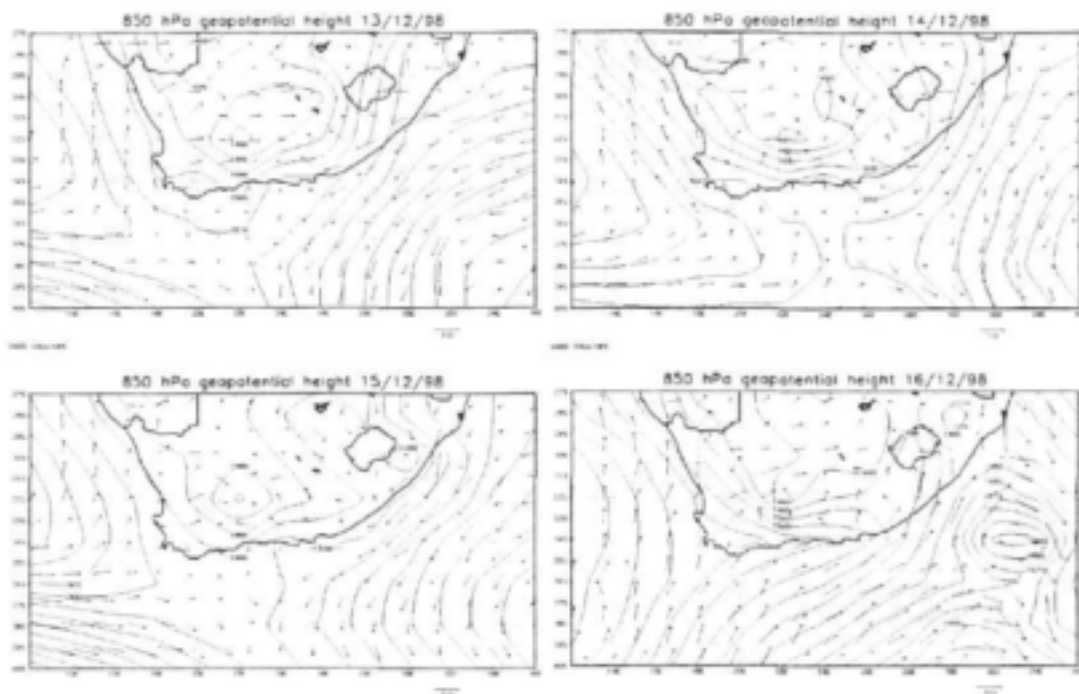
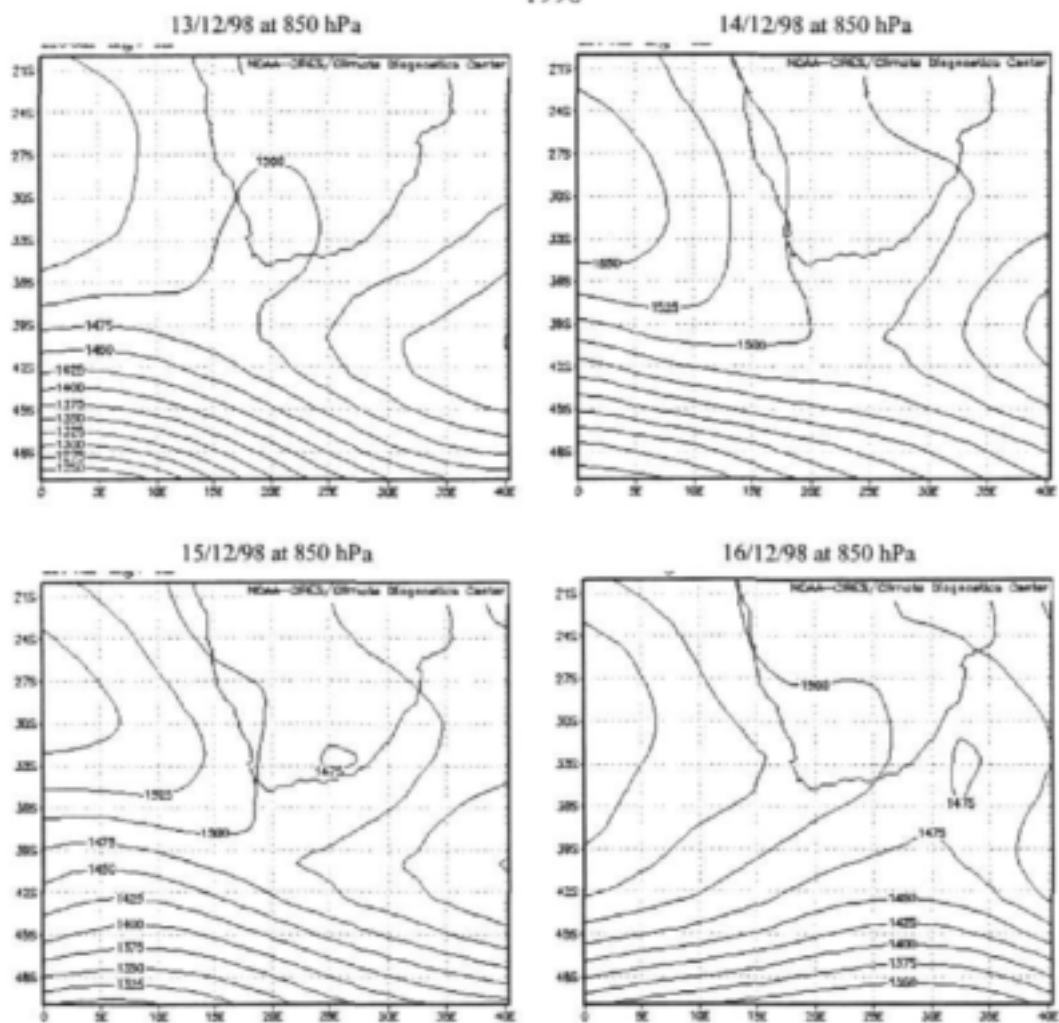


Figure 4.4 Model and NCEP 850 hPa geopotential height and winds 13 – 16 December 1998



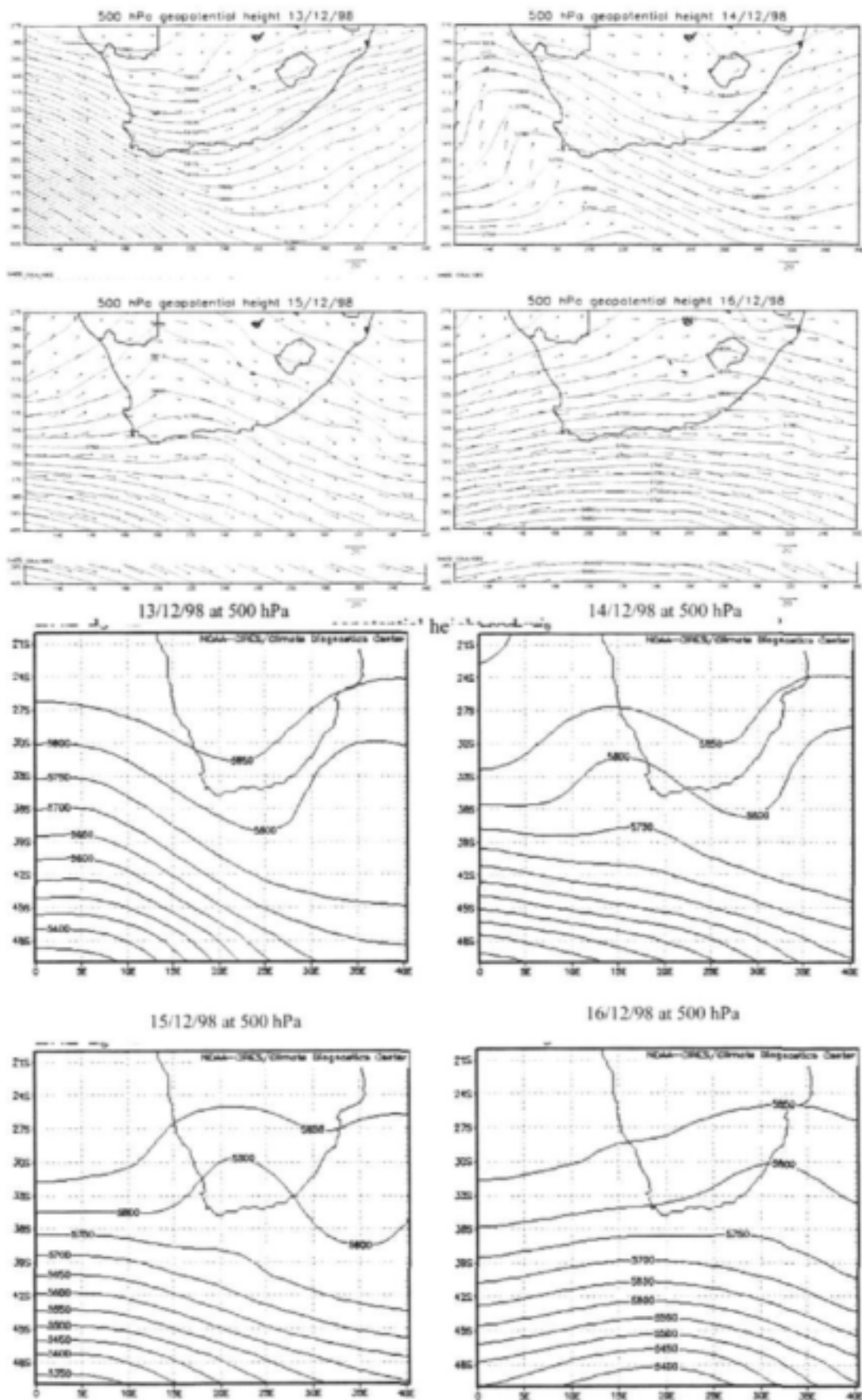


Figure 4.5 Model and NCEP 500 geopotential height for 13-16 December

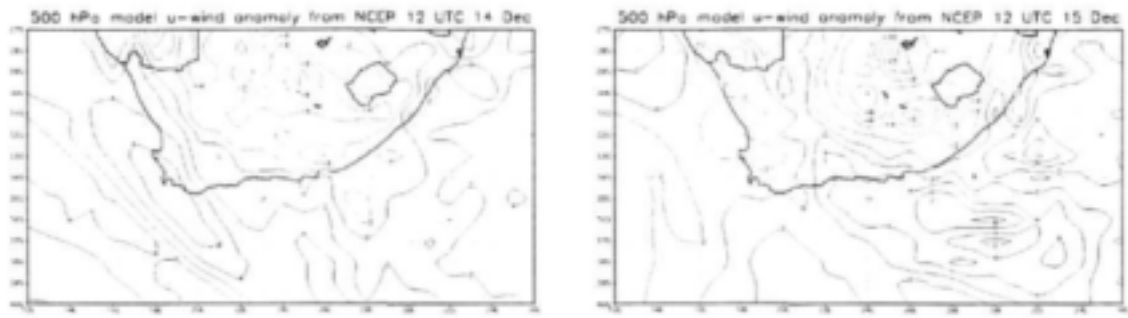


Figure 4.6 500 hPa u component of model wind anomalies from NCEP

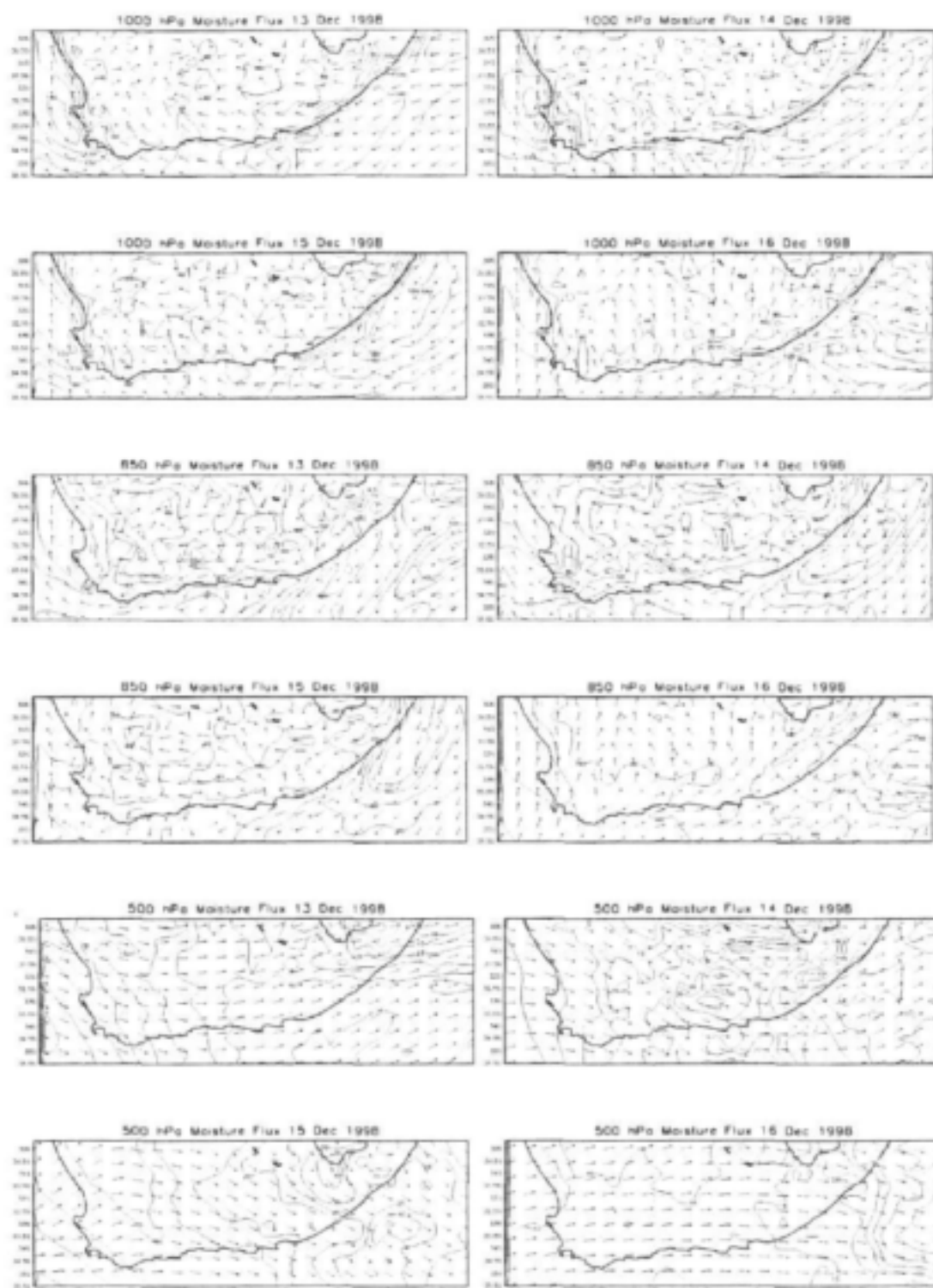


Figure 4.7 Model moisture fluxes ($\text{g}\cdot\text{kg}^{-1}\cdot\text{m}\cdot\text{s}^{-1}$) 13 – 16 December 1998 at 1000, 850 and 500 hPa

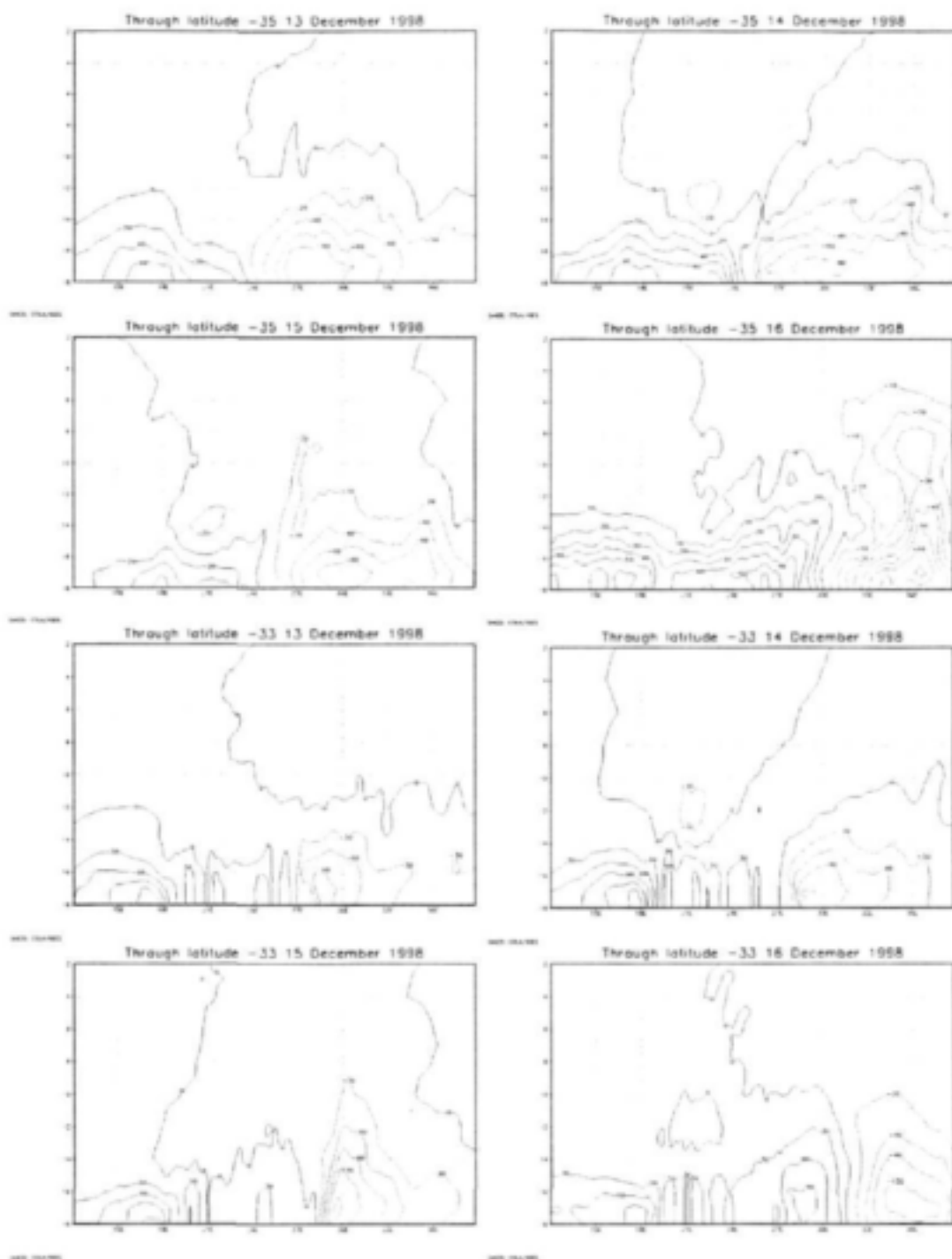
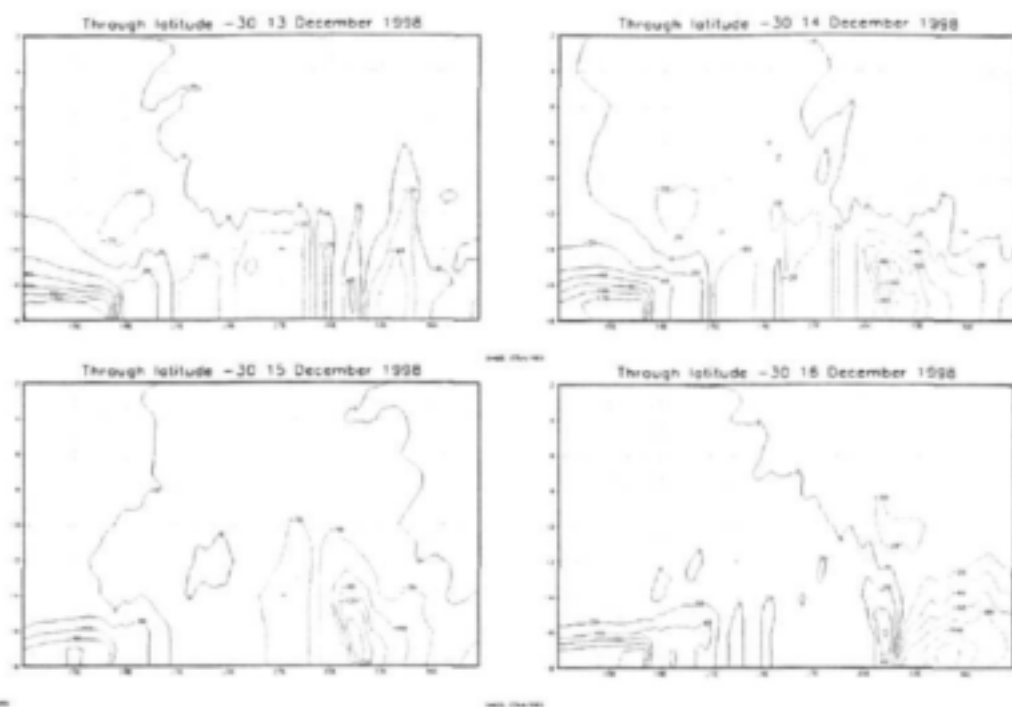


Figure 4.8 Vertical cross sections of model moisture fluxes ($\text{g.kg}^{-1} \text{m.s}^{-1}$) 13 – 16 December 1998 at 35, 33 and 30°S



(Figure 4.8 – cont.)

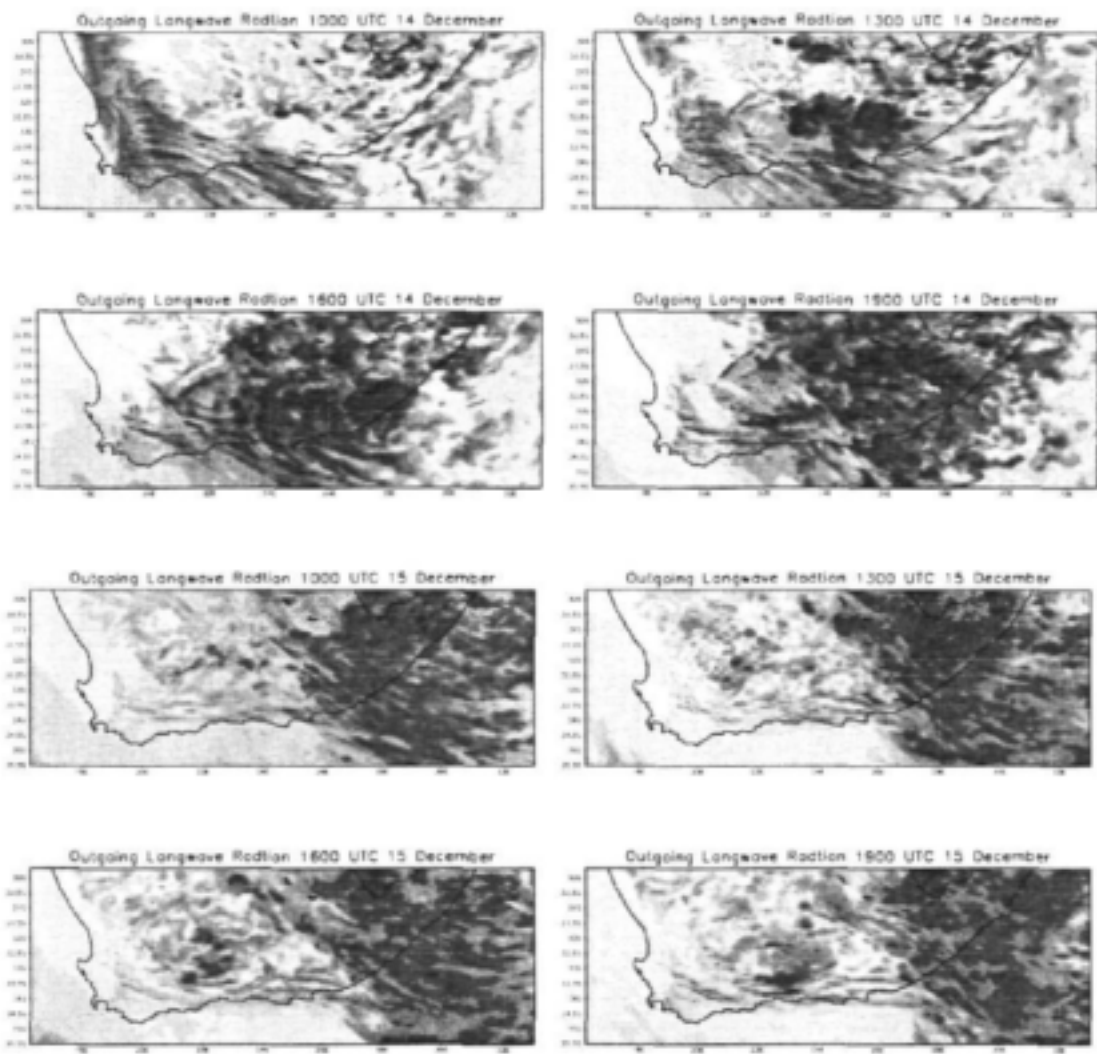


Figure 4.9 Model outgoing long wave radiation. Darker grey indicates areas of heavier cloud

5. Conclusion and recommendations

The major findings of the ocean and atmospheric modelling detailed above can be listed as follows:

1. The Agulhas Current region is highly variable on intraseasonal through to interdecadal scales. This variability implies significant anomalies in sea surface temperature, ocean heat content and transport, local evaporation and moisture fluxes, and hence in regional weather and climate patterns over South Africa.
2. Atmospheric general circulation model experiments have confirmed earlier observational work suggesting that South African summer rainfall is sensitive to sea surface temperature anomalies in the Agulhas Current region.
3. Mesoscale atmospheric model experiments confirm that moisture uptake over the Agulhas Current region may significantly influence severe weather over at least the southern part of South Africa.

The research emphasizes the need for South Africa to better monitor and understand its neighbouring oceans, particularly the Indian Ocean from where much of the moisture flux feeding into summer rainfall producing weather systems arises. Local forcing from the SW Indian Ocean is undeniably important but so are large scale near-global modes such as ENSO and other remote forcings (e.g. ocean teleconnections via the Indonesian throughflow, atmospheric teleconnections via Rossby wave signals emanating from areas of strong tropical convection). Being a relatively narrow subcontinent in an ocean dominated environment, southern Africa poses great challenges for better understanding of its climate variability and for improving seasonal forecasting capabilities. Crucial to these activities is ongoing support of observational and modelling research by South African funding agencies.

6. Refereed publications to which this project contributed

- Allan, R.J., C.J.C. Reason, J.A. Lindesay, T.J. Ansell, 2002: Protracted ENSO episodes over the Indian Ocean region. *Deep-Sea Res. II*, Special Issue on Oceanography of the Indian Ocean, accepted.
- Reason, C.J.C., C.R. Godfred-Spenning, R.J. Allan and J.A. Lindesay, 1998: Air-sea interaction mechanisms and low frequency climate variability in the South Indian Ocean region. *Int. J. Climatology*, 18(4), 391-405.
- Reason, C.J.C. and J.R.E. Lutjeharms, 1998: Variability of the South Indian Ocean and implications for southern African rainfall. *South African J. Sci.*, 94, 115-122.
- Reason, C.J.C. and C.R. Godfred-Spenning, 1998: SST variability in the South Indian Ocean and associated circulation and rainfall patterns over southern Africa. *Met. Atmos. Phys.*, 66, 243-258.
- Reason, C.J.C., 1998: Warm and cold events in the southeast Atlantic / southwest Indian Ocean region and potential impacts on circulation and rainfall over southern Africa. *Meteorol. Atmos. Phys.*, 69, 49-65.
- Reason, C.J.C., 1999: Interannual warm and cool events in the subtropical / mid-latitude South Indian Ocean region. *Geophys. Res. Lett.*, 26, 215-218.
- Reason, C.J.C. and H.M. Mulenga, 1999: Relationships between South African rainfall and SST anomalies in the South West Indian Ocean. *Int. J. Climatol.*, 19, 1651-1673.
- Reason, C.J.C., 2000: Multidecadal climate variability in the subtropics / midlatitudes of the Southern Hemisphere oceans. *Tellus*, 52A, 203-223.
- Reason, C.J.C., and J.R.E. Lutjeharms, 2000: Modelling multidecadal variability in the South Indian Ocean region: local forcing or a near-global mode? *S. Afr. J. Sci.*, 96, 127-134.
- Reason, C.J.C., R.J. Allan, J.A. Lindesay and T.J. Ansell, 2000: ENSO and climatic signals across the Indian Ocean basin in the global context: Part I, interannual composite patterns. *Int. J. Climatol.*, 20, 1285-1327.
- Reason, C.J.C. and R. Murray, 2001: Modelling low frequency variability in Southern Hemisphere extra-tropical cyclone characteristics and sensitivity to sea surface temperature. *Int. J. Climatol.*, 21, 249-267.
- Reason, C.J.C., K. Tory and P.L. Jackson, 2001: Models of coastally trapped

- disturbances: validations from realistic simulations. *J. Atmos. Sci.*, 58, 1892-1906.
- Reason, C.J.C., 2001: Evidence for the influence of the Agulhas Current on regional atmospheric circulation patterns. *J. Clim.*, 14, 2769-2778.
- Reason, C.J.C., 2001: Subtropical Indian Ocean SST dipole events and southern African rainfall. *Geophys. Res. Lett.*, 28, 225-228.
- Reason, C.J.C. and M. Rouault, 2002: ENSO-like decadal patterns and South African rainfall. *Geophys. Res. Lett.*, 29 (13), 16-1 – 16-4.
- Reason, C.J.C., and P.L. Jackson, 2002: Modelling a southeast Australian coastal ridging event. *Meteorol. Applic.*, 9, 383-397.
- Reason, C.J.C., 2002: Sensitivity of the southern African circulation to dipole SST patterns in the South Indian Ocean. *Int. J. Climatol.*, 22, 377-393.
- Reason, C.J.C., 2002: The wet 2001 winter over the SW Cape: potential large scale influences. *S. Afr. J. Sci.*, 98, 307-310.
- Reason, C.J.C., M. Rouault, J.-L. Melice and D. Jagadeesha, 2002: Interannual winter rainfall variability in SW South Africa and large scale ocean-atmosphere interactions. *Met. Atmos. Phys.*, Special Issue on *Atmosphere-surface interactions*, 80 (1-4), 19-29.
- Reason, C.J.C., J.R.E. Lutjeharms, J. Hermes, A. Biastoch and R. Roman 2003: Inter-ocean exchange south of Africa in an eddy-permitting model. *Deep-Sea Res. II*, Special Issue on KAPEX, 50, 281-298.
- Rouault, M., S.A. White, C.J.C. Reason and J.R.E. Lutjeharms, 2002: Ocean-Atmosphere Interaction in the Agulhas Current and a South African extreme weather event. *Weather and Forecasting*, 17, 655-669.
- Rouault, M., P. Florenchie, N. Fauchereau and C.J.C. Reason, 2003: South East Atlantic warm events and southern African rainfall. *Geophys. Res. Lett.*, in press.
- Rouault, M., C.J.C. Reason, J.R.E. Lutjeharms and A. Beljaars, 2003: Underestimation of latent and sensible heat fluxes above the Agulhas Current in NCEP and ECMWF analyses. *J. Clim.*, 16, 776-782.

Other related WRC reports available:

Air-Sea interaction over the Agulhas Current and implication for South African weather

Rouault M • Lutjeharms JRE • Lee-Thorp AM • Jury MR • Majodina M

Previous investigations have revealed that the oceanic environment of Southern Africa plays an important regulating role in the climate of the subcontinent. In particular, statistical teleconnections between oceanic temperature anomalies and precipitation over South Africa's summer rainfall region have been demonstrated. This research project was designed to investigate the physical mechanisms of ocean-atmosphere interaction as a means of contributing to a better understanding of the role of the oceans in affecting the weather of the subcontinent. The Agulhas Current region was selected as the study area.

The first task was to assemble and test a portable micrometeorological instrumentation system required to make the necessary on-board ship measurements in order to quantify the turbulent exchanges of water vapour, heat and momentum above the ocean surface. Measurements obtained at ship level could then be linked to measurements at other levels in the atmosphere through the use of radiosondes. Considerable difficulties had to be overcome before the instrumentation could be used successfully to obtain the necessary high-quality data. A large volume of data were collected during several cruises undertaken over the five-year research period. Among the many results was the finding that the core of the Agulhas Current, about 50 km wide, transfers about 5 times as much water vapour to the atmosphere as the surrounding water, all year long.

The instrumentation and expertise developed during the course of this project, when used in conjunction with satellite remote sensing, should provide the means of extending the quantification of air-sea interactions to much larger surrounding ocean areas than have up to now been investigated. This will greatly benefit the further development of atmospheric circulation models and add to the understanding of the mechanisms whereby the surrounding oceans affect the climate of South Africa

Report Number: 374/1/99

ISBN: 1 86845 489 4

<p>TO ORDER: Contact Rina or Judas - Telephone No: 012 330 0340 Fax Number: 012 331 2565 E-mail: publications@wrc.org.za</p>

Water Research Commission
Private Bag X03, Gezina, 0031, South Africa
Tel: +27 12 330 0340, Fax: +27 12 331 2565
Web: <http://www.wrc.org.za>

